Resolving ecological feedbacks on the ocean carbon sink in Earth system models

David I. Armstrong M^{c}Kay*[1,2], Sarah E. Cornell[1,2], Katherine Richardson[3], Johan Rockström[1,4]

[1]Stockholm Resilience Centre, Stockholm University, Stockholm, 106 91, Sweden
[2]Bolin Centre for Climate Research, Stockholm University, Stockholm, 106 91, Sweden
[3]Globe Institute, Center for Macroecology, Evolution and Climate, University of Copenhagen, Copenhagen, 2100, Denmark
[4]Potsdam Institute for Climate Impact Research, Potsdam, 14473, Germany

Correspondence to: David I. Armstrong M^{c}Kay (david.armstrongmckay@su.se)

Abstract. The Earth's oceans are one of the largest sinks in the Earth system for anthropogenic CO_2 emissions, acting as a negative feedback on climate change. Earth system models predict that climate change will lead to a weakening ocean carbon uptake rate as warm water holds less dissolved CO_2 and biological productivity declines. However, most Earth system models do not incorporate the impact of warming on bacterial remineralisation and rely on simplified representations of plankton ecology that do not resolve the potential impact of climate change on ecosystem structure or elemental stoichiometry. Here we use a recently-developed extension of the cGEnIE Earth system model (ecoGEnIE) featuring a trait-based scheme for plankton ecology (ECOGEM), and also incorporate cGEnIE's temperature-dependent remineralisation (TDR) scheme. This enables evaluation of the impact of both ecological dynamics and temperature-dependent remineralisation on the soft-tissue biological pump in response to climate change. We find that including TDR strengthens the biological pump relative to default runs due to increased nutrient recycling, while ECOGEM weakens the biological pump by enabling a shift to smaller plankton classes. However, interactions with carbonate chemistry cause opposite sign responses for the carbon sink in both cases: TDR leads to a smaller sink relative to default runs whereas ECOGEM leads to a larger sink. Combining TDR and ECOGEM results in a net strengthening of the biological pump and a small net reduction in carbon sink relative to default. These results illustrate the substantial degree to which ecological dynamics and biodiversity modulate the strength of the biological pump, and demonstrate that Earth system models need to incorporate ecological complexity in order to resolve climate-biosphere feedbacks.

1. Introduction

Oceans absorb about a quarter of anthropogenic carbon dioxide emissions, drawing down around 2-3 $PgCy^{-1}$ in recent decades (Ciais et al., 2013; Friedlingstein et al., 2019; Gruber et al., 2019). The mechanisms of carbon sink processes are well understood: solubility (dissolution) and biological (soft tissue and hard carbonate) pumps transfer carbon to the deep ocean where it remains on timescales of several centuries to millennia (Broecker and Peng, 1982). However, increasing ocean temperature as a result of global warming could potentially lead to a weakening of this ocean carbon sink (Arora et al., 2013;

Ciais et al., 2013). The global carbon sink uptake rate was observed to decline by ~0.91%yr^{-1} between 1959 and 2012, of which approximately 40% is estimated to be due to feedback responses of sink processes (nonlinear carbon-cycle responses to CO_2 and carbon–climate coupling) with the oceans playing a large role (Raupach et al., 2014). The combined effect of future feedbacks on both land and ocean carbon sinks reduce the RCP4.5-compatible anthropogenic carbon budget by ~157 ± 76 PgC (Ciais et al., 2013).

This sink weakening might therefore act as a positive feedback on anthropogenic warming (Steffen et al., 2018). However, many of the Earth system models (ESMs) used to make these carbon sink projections do not incorporate sufficient ecological complexity to fully resolve these feedbacks, including for the ocean the impact of both warming and acidification on metabolic dynamics, ecosystem structure, and nutrient stoichiometry (Ciais et al., 2013). Of the ten ESMs from the Coupled Model Intercomparison Project Phase 5 (CMIP5) used for carbon sink projections in the fifth assessment report of the Intergovernmental Panel on Climate Change (IPCC AR5), only one resolves the impact of warming on organic carbon remineralisation, three resolve different plankton sizes, and three resolve changing nutrient usage ratios (discussed in Background below), all of which critically influence the biological pump in a warming ocean. While there have been some improvements in the next generation CMIP6 ESMs, most still use a fixed remineralisation parameterisation for exported organic carbon and feature broad size classes rather than a full spectrum of plankton size classes.

In this study we investigate changes in the biological pump in response to climate change and ocean acidification using ecoGEnIE, an ESM of intermediate complexity (EMIC) with more complex biogeochemistry and ecosystem dynamics than present in most CMIP ESMs. The ecoGEnIE model allows temperature-dependent remineralisation, greater biodiversity via size trait-based plankton ecology, and flexible elemental stoichiometry. This combination allows the impact of metabolic and ecological dynamics on the biological pump and the ocean carbon sink in response to climate change to emerge, while the choice of an EMIC makes such additional complexity computationally tractable. We simulate a suite of historical and future climate change scenarios and assess the impact on the ocean carbon sink of replacing the default remineralisation parameterisation with the temperature-dependent scheme and/or the parameterised biogeochemistry module with ecoGEnIE's new explicit trait-based plankton ecology scheme.

This manuscript is structured as follows. In section 2 we give detailed background on the role of the biological pump, how it may be affected by climate change and ocean acidification, and to what extent current Earth system models resolve these effects. In section 3 we describe the ecoGEnIE model and our experimental setup. In section 4 we describe the results of our experiments, focusing on the contrasting results for biological pump strength and the ocean carbon sink across the different model configurations. And finally in section 5 we discuss the implications and limitations of our results.

2. Background

The primary driver of a weakening ocean carbon sink in response to anthropogenic climate change is the reduced CO_2 dissolution capacity of warmer water (i.e. a weaker solubility pump), but changes in the biological pump modulate this physicochemical process by affecting the vertical partitioning of carbon within the ocean. In general Earth system models project a weakening of the biological pump as a result of ocean stratification reducing nutrient availability (Bopp et al., 2013), but a reduced efficacy of the biological pump due to increased marine bacterial respiration has also been suggested as an important factor in past warm episodes (Boscolo-Galazzo et al., 2018; John et al., 2014a; Olivarez Lyle and Lyle, 2006).

[Figure 1]

The biological pump describes the fixation and export of carbon and nutrients from the surface to the poorly ventilated deep ocean by biological activity. The vast majority of this organic matter is remineralised as it sinks and is later gradually returned in dissolved form to surface waters by ocean upwelling (Figure 1). The formation and export of calcium carbonate shells (Particulate Inorganic Carbon; PIC) also forms part of the biological pump, but hereafter we focus on the soft-tissue biological pump as it is the dominant driver of surface carbon export (Dunne et al., 2007).

After organic carbon is fixed in the surface euphotic layer by phytoplankton and some is consumed by zooplankton, Particulate Organic Matter (POM) begins to be remineralised by detritivorous bacteria as it falls through the water column as POM rain. Most POM is remineralised to Dissolved Organic Matter (DOM) within the epipelagic mixed layer (~0-200m) where the nutrients released are rapidly recycled into 'regenerated' production (Dugdale and Goering, 1967) and in the mesopelagic zone (~200-1000m) below, but up to 4-12 $PgCy^{-1}$ of Particulate Organic Carbon (POC) leaves the surface ocean (Ciais et al., 2013; Dunne et al., 2007; Henson et al., 2011, 2012; Mouw et al., 2016a). This remineralisation profile follows a power law distribution, with a rapid geometric decline in export flux from the base of the mixed layer to a small asymptotic flux by ~1000m. Once in the poorly ventilated deep ocean, the surviving POM (most of which is subsequently remineralised to DOM) remains on centennial-to-millennial timescales before being eventually returned to the surface by upwelling, while a tiny fraction of mostly recalcitrant POM is buried in sediment and so sequestered on geological timescales.

The simplified representation of plankton ecology and the biological pump shown in Figure 1 forms the basis of many marine biogeochemical models, such as the one-size fixed-trait phyto- and zooplankton classes in the common NPZD (Nutrient-Phytoplankton-Zooplankton-Detritus) scheme (Friedrichs et al., 2007; Kwiatkowski et al., 2014). This approach misses many important biogeochemical processes though, prompting the development of 'dynamic green ocean models' which introduce multiple Plankton Functional Types (PFTs) with differentiated biogeochemical roles (Aumont et al., 2003; Quere et al., 2005). However, this class of plankton model is still limited by a profusion of poorly constrained parameters based on limited

observations, taxonomic overspecificity, and still-limited representation of biodiversity (Anderson, 2005; Boscolo-Galazzo et al., 2018; Friedrichs et al., 2007; Shimoda and Arhonditsis, 2016; Ward et al., 2018).

Although significant progress has been made since IPCC AR5 in optimising biogeochemical and ecological parameterisations in both NPZD and dynamic green ocean models using novel data assimilation and statistical techniques (Chien et al., 2020; Frants et al., 2016; Kriest, 2017; Kriest et al., 2020; Niemeyer et al., 2019; Sauerland et al., 2019; Schartau et al., 2017; Yao et al., 2019), neither approach fully accounts for allometric effects in biogeochemistry. Cell size distribution and elemental stoichiometry are dominant traits controlling plankton ecosystem function and total production (Finkel et al., 2010; Guidi et al., 2009) and projections indicate that the fraction of large phytoplankton will increase with nutrient availability and decrease with warming (Mousing et al., 2014). Plankton size also has a substantial effect on POC export efficiency, with observations and models suggesting that although smaller plankton favour a greater proportion of POC being exported from the surface layer this POC dominated by small, slow sinking particles degrades more rapidly in the mesopelagic zone (Leung et al., 2021; Mouw et al., 2016b; Omand et al., 2020; Weber et al., 2016). Trait-based plankton models have been proposed to cover this allometric gap, based on simulating generic ecosystem rules using key functional traits such as size rather than specific taxonomic identity, allowing ecosystem structure, biodiversity, and biogeography to emerge without being parameterised (Bruggeman and Kooijman, 2007; Follows et al., 2007; Harfoot et al., 2014; McGill et al., 2006). These ecosystem models still do not enable better understanding of Earth system feedbacks though because they have not been systematically incorporated into ESMs and so do not capture wider biogeochemical and large-scale physical dynamics.

Most biogeochemical models feature fixed phytoplankton stoichiometry, often following the canonical Redfield ratio for C:N:P of 106:16:1 or similar (Martiny et al., 2014; Redfield, 1934). However, real organisms can deviate substantially from this ratio, depending on cell size, functional group. and environmental conditions, with the Redfield ratio only emerging on a wider scale (Finkel et al., 2010). Climate change and ocean acidification are expected to substantially change ecosystem composition and nutrient availability, while increasing temperatures and CO_2 concentrations have a direct impact on nutrient assimilation (Martiny et al., 2016; Moreno and Martiny, 2018; Riebesell et al., 2009). The C:P ratio has also been observed to increase with decreasing P availability as phytoplankton increased their P usage efficiency, which could help maintain production and therefore export despite expansion of low-nutrient oligotrophic zones ('oligotrophication') (Galbraith and Martiny, 2015). It is therefore likely that stoichiometry of POC may change in response to ocean warming and acidification, with potential knock-on effects for the efficacy of the biological pump as a whole (Moreno et al., 2018). Despite this, flexible stoichiometry – with nutrient uptake by phytoplankton depending on current availability and their current cell quota – is rarely incorporated in ocean biogeochemistry models (Ward et al., 2018).

Metabolic processes are also temperature-dependent, and so ocean temperature partly determines many marine biogeochemical patterns (Hoppe et al., 2002; Laws et al., 2000; Regaudie-De-Gioux and Duarte, 2012). For every 10^{o}C increase in temperature,

photosynthesis in any location is expected to increase by up to 100% (represented by a Q10 factor of 1-2), while average community respiration is expected to increase by between 100 and 200% (Q10 = 2-3) (Bendtsen et al., 2015; Boscolo-Galazzo et al., 2018; Eppley, 1972; Pomeroy and Wiebe, 2001; Regaudie-de-Gioux and Duarte, 2012; Sarmento et al., 2010). If warming-induced increases in respiration rates rise faster than production rates, organic matter will be remineralised more quickly, shoaling the remineralisation depth (the e-folding point at which ~63% of POC is remineralised) (Boscolo-Galazzo et al., 2018; John et al., 2014a; Kwon et al., 2009) and may also reduce transfer efficiency within the mesopelagic zone (Fakhraee et al., 2020; Weber et al., 2016). One might expect this to reduce carbon export overall as less carbon makes it out of the surface ocean, but increased remineralisation also allows more nutrients to be recycled back into the surface, potentially resulting in more regenerated production (Leung et al., 2021; Segschneider and Bendtsen, 2013; Taucher and Oschlies, 2011). Even a small shift in the remineralisation depth could have a significant potential impact on atmospheric CO_2, potentially acting as a positive climate feedback mechanism. For example, a global deepening of 24m (for example as a result of cooling) reduced CO_2 by 10-27 ppm in one model (Kwon et al., 2009). Although the biological pump itself does not act as a carbon sink in long-term equilibrium (as exported carbon is returned to the surface by upwelling on millennial timescales), a change in biological pump strength could create a transient carbon sink if it enables a higher equilibrium accumulation of carbon in the deep ocean.

Other processes that affect the biological pump and remineralisation will also be impacted by climate change. Ocean stratification is projected to increase, as surface warming increases the temperature gradient (Ciais et al., 2013; Riebesell et al., 2009). This reduces the nutrient flux from deep to surface waters, potentially leading to oligotrophication in lower latitude surface waters (Bopp et al., 2005; Sarmiento et al., 2004). Oligotrophication leads to lower overall productivity in productive regions, but warming will not substantially affect productivity in existing oligotrophic regions where production is already limited (Richardson and Bendtsen, 2017). Oligotrophic regions may also be more productive than expected due to continued sub-surface production in deep chlorophyll maxima, but most ESMs do not resolve this phenomenon (Richardson and Bendtsen, 2019). The reduction in nutrient supply may also favour smaller plankton that can better cope with warmer and oligotrophic conditions, resulting in a shift in ecosystem dynamics and function (Beaugrand et al., 2010; Bopp et al., 2005; Finkel et al., 2010). Reduced mixing rates along with surface warming also results in ocean interior deoxygenation, leading to an expansion of oxygen minimum zones, reduced nitrogen availability due to increasing denitrification, and increased phosphate release from affected sediments (Ciais et al., 2013; Keeling et al., 2010; Stramma et al., 2008).

The organic biological pump may also be affected by ocean acidification through shifting ecosystem composition, altered nutrient availability, and stoichiometric effects (Ciais et al., 2013; Nagelkerken and Connell, 2015; Riebesell et al., 2009; Tagliabue et al., 2011). Acidification may increase the C:N uptake ratio and decrease the N:P uptake ratio, potentially making production more efficient (Riebesell et al., 2007; Tagliabue et al., 2011). Acidification could also lead to reduced particle ballasting – the hypothesised process by which denser falling PIC protects associated POC and so increases POC export – by

reducing the supply of PIC and therefore reducing the efficiency of POC export (Armstrong et al., 2001; Klaas and Archer, 2002). However, the overall effect of ocean acidification feedbacks remains uncertain (Doney et al., 2020), and many of these processes are not resolved by ESMs. Furthermore, the human-driven loss of organisms higher up the food chain as a result of overharvesting and habitat degradation has a considerable yet poorly quantified effect on the biological pump (Pershing et al., 2010). Many of these factors influence and/or are influenced by both the magnitude of primary production and the remineralisation depth.

[Table 1]

Despite these known influences on the biological pump, many of the ESMs used for the IPCC AR5's ocean carbon sink projections incorporated few if any of these biogeochemical processes (Ciais et al., 2013; Schwinger et al., 2014). One study (Segschneider and Bendtsen, 2013) quantified the impact of including TDR, modifying the CMIP5 model MPI-ESM and its marine biogeochemistry model HAMOCC5.2, and projected an ~18 PgC reduction in ocean carbon uptake by 2100 under high emission scenario RCP8.5. However, only one out of ten CMIP5 ESMs featured non-fixed POC remineralisation profiles by enabling TDR (CanESM2) (Table 1), with most instead prescribing a fixed attenuating remineralisation profile with vertical POC flux following modern ocean observations (sometimes called the 'Martin Curve' (Bendtsen et al., 2015; Dunne et al., 2007; Martin et al., 1987)). Additionally, NPZD-type models cannot fully resolve the potential impact of climate change or ocean acidification on ecosystem structure, biodiversity, and plankton size shifts as they do not resolve allometric or stoichiometric effects. Only four of the ten CMIP5 ESMs featured multiple PFTs with different ecosystem functions beyond a simple NPZD scheme. Of these, only three account for plankton size in some way, and only three featured at least partially flexible stoichiometry (e.g. nutrient quotas and optimal allocation) that allow potential changes in nutrient utilisation in response to changing environmental conditions to be resolved (Kwiatkowski et al., 2018; Moreno and Martiny, 2018).

The next generation of CMIP6 ESMs for IPCC AR6 are currently in the process of completion, so insufficient results are available for use as comparison in this study. These models show some improvements in these regards, with five models reporting an increase in the number of explicit or implicit PFT or bacteria classes, three models introducing more variable stoichiometry (although one model has instead reduced flexible stoichiometry), and two models introducing more than one sinking POC classes (Séférian et al., 2020). Despite these improvements, the CMIP6 models still only feature broad size classes rather than a full spectrum of plankton size classes, only three have fully flexible stoichiometry, and most still use a fixed remineralisation profile for exported POC. Investigating changes in the biological pump in response to the physical and chemical perturbations of climate change and ocean acidification therefore requires an ESM with more complex biogeochemistry and ecosystem dynamics than present in these ESMs.

3. Methods

3.1. The cGEnIE model

ecoGEnIE is an extension of cGEnIE – the carbon-centric Grid Enabled Integrated Earth system model, an EMIC based on a modular framework efficiently resolving ocean circulation, biogeochemistry, and optional deep-sea sediment that has been simplified to focus on long-term carbon cycle (Ridgwell et al., 2007; Ridgwell and Schmidt, 2010). cGEnIE has been used in many previous studies of climate-carbon cycle interactions in both modern (Tagliabue et al., 2016) and palaeo applications (Gibbs et al., 2016; John et al., 2014a; Meyer et al., 2016; Monteiro et al., 2012; Norris et al., 2013; Ridgwell and Schmidt, 2010). EMICs such as cGEnIE have lower spatiotemporal resolution than more comprehensive ESMs based on atmosphere-ocean general circulation models and so are limited in their physical realism, but they are also less computationally expensive and thus well-suited for investigating more complex biogeochemical dynamics and performing efficient simulations of longer timescales or multiple scenarios (Claussen et al., 2002; Ward et al., 2018).

cGEnIE's climate model (C-GOLDSTEIN) features 3D reduced physics (frictional geostrophic, non-eddy resolving) ocean circulation model coupled to a 2D energy–moisture balance model of the atmosphere and a dynamic–thermodynamic sea-ice model (Edwards and Marsh, 2005; Marsh et al., 2011). C-GOLDSTEIN is configured on a 36 x 36 equal area horizontal grid (each cell being 10^{o} in longitude and varying from ~3.2^{o} to 19.2^{o} in latitude), has 16 logarithmically-spaced vertical layers, and 96 time steps per year. The horizontal and vertical transport of heat, salinity, and biogeochemical tracers is calculated via a combined parameterisation for isoneutral diffusion and eddy-induced advection. cGEnIE also features a comprehensive ocean biogeochemistry module (BIOGEM) with phosphorus (in the form of phosphate, PO_4) and iron as the co-limiting nutrients (Ridgwell et al., 2007; Ridgwell and Schmidt, 2010; Ward et al., 2018). Organic matter production and export is parameterised in BIOGEM as a function of nutrient availability and following a fixed dissolved to particulate organic matter (DOM:POM) ratio, while $CaCO_3$ production and export is parameterised by a saturation state-dependent particulate inorganic to organic carbon (PIC:POC) rain ratio. BIOGEM by default uses a fixed remineralisation profile similar to the Martin curve for the sinking labile fractions of both POC and PIC (Martin et al., 1987; Ridgwell et al., 2007), but includes an optional temperature-dependent remineralisation scheme which has previously been used to explore the biological pump in warm palaeo oceans (John et al., 2014b). An updated calibration of this scheme which also couples TDR with temperature-dependent export production was also recently developed (Crichton et al., 2021) and is the version (*cGEnIE.muffin* v0.9.13) used in this paper.

3.2. The ecoGEnIE extension

The current cGEnIE version (*cGEnIE.muffin*) has recently been extended to ecoGEnIE (v.1.0) by incorporating a new scheme for plankton ecology (ECOGEM), replacing cGEnIE's implicit, flux-based parameterisation biogeochemistry module BIOGEM with an explicitly resolved and temperature-sensitive trait-based ecosystem module (Ward et al., 2018). In contrast to BIOGEM, biomass is now explicitly resolved, with each plankton population subject to ecophysiological processes including nutrient uptake (subject to quota saturation), photosynthesis and oxygen production (subject to light limitation, photoacclimation, and seasonal light attenuation within a variable mixed layer depth), predation (subject to prey-switching, prey refugia, and prey assimilation), and mortality. Many of these processes are temperature-sensitive (nutrient uptake, photosynthesis, and predation) or size-dependent (maximum photosynthetic and nutrient uptake rates, nutrient affinities, cell carbon quotas, maximum prey ingestion rates, and DOM fraction). In this configuration of ecoGEnIE (v.1.0) there are two plankton functional types (PFTs) available: phytoplankton (with nutrient uptake and photosynthetic traits enabled) and zooplankton (with predation traits enabled), with further classes such as calcifiers and silicifiers to be made available in future. Explicitly resolving biomass also allows introduces a lag between environmental forcing and ecosystem response, allowing seasonal cycles and transient behaviour in POC production and export to emerge (Galbraith et al., 2015).

As size is the dominant trait controlling plankton biogeochemical function and response to warming (Finkel et al., 2010; Mousing et al., 2014) each PFT is further split into 8 size classes ranging from 0.6μm to 1900μm. Zooplankton graze on all potential prey subject to availability with an optimum predator:prey length ratio of 10. This allows a better resolution of biodiversity within the model relative to models without size classes, with the ecosystem capable of shifting to a different structure in response to environmental forcing. ECOGEM also includes flexible stoichiometry rather than being fixed to the canonical Redfield ratio, allowing dynamic usage of nutrients in response to warming, ocean acidification, and nutrient availability to also be resolved (Boscolo-Galazzo et al., 2018; Martiny et al., 2016; Moreno and Martiny, 2018). DOM production is explicit in ECOGEM and so allows a variable and plankton size-dependent POM:DOM ratio, variations in which may have a significant impact on primary production in oligotrophic regions (Richardson and Bendtsen, 2017) and would result in reduced POM export with a shift to smaller plankton classes.

Although using an EMIC such as cGEnIE/ecoGEnIE allows for greater ecological resolution, it introduces different limitations. cGEnIE/ecoGEnIE has coarse spatial (36 x 36 equal area horizontal grid and 16 ocean layers) and temporal resolution (every ~4 days for C-GOLDSTEIN, every ~8 days for BIOGEM, and every ~0.4 days for ECOGEM), and so is not able to fully resolve spatial circulation and ecological patterns, vertical POC distribution, or the dynamics that potentially link stratification and deep chlorophyll maxima in oligotrophic regions (Richardson and Bendtsen, 2017, 2019). Subtle differences in spatial resolution and physical framework representations can have a substantial impact on circulation patterns, which could affect plankton community structure and the residence time of exported nutrients and carbon (Pasquier and Holzer, 2016; Sinha et

al., 2010). Currently only two PFTs are available in ecoGEnIE (phytoplankton and zooplankton, with PIC export set as saturation state-dependent ratio of POC), limiting the extent to which hard pump dynamics involving calcifiers and silicifiers can emerge in our results. ecoGEnIE has not yet been fully recalibrated to the modern ocean and does not perform quite as well against observational data for key biogeochemical tracers (DIC, ALK; PO_4, O_2) as cGEnIE (Ward et al., 2018), but the results are still broadly similar (reproducing approximately 90% of the global variability in DIC, more than 70% for PO_4, O_2, and ALK, and more than 50% for surface chlorophyll, and broadly captures vertical distributions of these tracers). In this study we focus primarily on the global biological pump response rather than its spatial patterns, and are also particularly concerned with surface DIC and its relation to ocean carbon sink dynamics, and so this configuration is sufficient for this global analysis.

3.3. Experimental setup

We assess the differing impacts of replacing cGEnIE's Fixed Profile Remineralisation (FPR) parameterisation with its Temperature-Dependent Remineralisation (TDR) scheme (John et al., 2014b) and replacing cGEnIE's original parameterised biogeochemistry BIOGEM module (BIO) with ecoGEnIE's trait-based ECOGEM module (ECO) (Ward et al., 2018). We test each new element both separately and in combination, analysing four cGEnIE/ecoGEnIE configurations:

- **BIO+FPR** is cGEnIE with the default BIOGEM module (BIO) and the default Fixed Profile Remineralisation scheme (FPR)
- **BIO+TDR** is cGEnIE with the default BIOGEM module (BIO) and the alternative Temperature-Dependent Remineralisation scheme (TDR)
- **ECO+FPR** is ecoGEnIE, incorporating the trait-based ECOGEM module with flexible stoichiometry (ECO), and the default Fixed Profile Remineralisation scheme (FPR)
- **ECO+TDR** is ecoGEnIE (ECO) and the alternative Temperature-Dependent Remineralisation scheme (TDR)

We use the global POC export flux ($PgCy^{-1}$) from the surface layer (fixed in cGEnIE/ecoGEnIE as the top 80.8m of the ocean, compared with ~100m in some studies (Martin et al., 1987)) as our measure of biological pump strength and compare cumulative changes up to the year 2100 CE, and also quantify cumulative changes in the ocean carbon sink for each configuration through the air-to-sea CO_2 flux. We calculate cumulative changes in biological pump and ocean carbon sink capacity for the policy-relevant timescale of the 21st Century CE (Table 2), but results are also shown up to 2500 CE (Figure 2).

Each configuration is run both under its default published calibration and recalibrated to result in the same preindustrial global biological pump strength (POC export of ~7.5 $PgCy^{-1}$ and PIC export of ~1 $PgCy^{-1}$) and similar global mean total Dissolved Inorganic Carbon (DIC), Alkalinity (ALK), and surface DIC speciation relative to the BIO+FPR and observational data (see Supplementary Table S1 & Figures S1-S44). The configurations were recalibrated to have as similar a carbon cycle as possible in order to make the results easily comparable across the configurations, while POC export was chosen as the primary calibration constraint as the main variable being analysed. However, some differences remain between the recalibrated configurations as well as with the observational data. The main difference is a higher POC sedimentation rate in the ECO configurations as a result of specifying a higher recalcitrant fraction (from ~5% to ~32-35%) in order to counter much high POC export in ecoGEnIE. Although this recalcitrant fraction and the resulting POC rain rate is unrealistically high compared to observations, in cGEnIE recalcitrant POC remains inert until sedimentation and so does not directly interact with the rest of the carbon cycle. POC rain in sediment module-disabled configurations of cGEnIE is returned as deep ocean DIC and nutrients upon reaching the sea floor, meaning total ocean DIC is still conserved and biological pump perturbations on sub-overturning timescales (<500-1000y) will not significantly affect surface DIC within that time. Optimising for equivalent POC export also leads to surface carbonate concentration ($[CO_3]$) being reduced in BIO+TDR compared with the default calibration, leading to a reduced carbonate buffer for the ocean carbon sink in these runs. To constrain the impact of these calibrations on our results, we also present default calibration results in the Supplementary Material and discuss the differences in our Results.

Each model configuration is spun-up for 10,000 years and restarted at 0 CE (10000 Holocene Era, HE), and then forced in emissions mode from 1765 CE with combined historical and future CMIP5 RCP total CO_2 emission scenarios (3PD, 4.5, 6.0, and 8.5, corresponding to low, moderate, high, and severe emission scenarios respectively; 3PD used instead of RCP2.6 to allow for long-term simulation beyond 2100 CE) extended through to 2500 CE in order to assess multi-centennial dynamics (Meinshausen et al., 2011).

4. Results

4.1. Physical Climate Response

In its default configuration (BIO+FPR) cGEnIE projects surface air temperature warming of 1.8ºC, 2.6ºC, 3.2ºC, and 4.2ºC by 2100 relative to 1850-1900 in RCPs 3PD, 4.5, 6.0, and 8.5 respectively, which compares favourably with CMIP5 projections for these scenarios (1.6ºC±0.4ºC, 2.4ºC±0.5ºC, 2.8ºC±0.5ºC, and 4.3ºC±0.7ºC) (Collins et al., 2013). In the ocean, cGEnIE-BIO+FPR projects sea surface warming of 1.2ºC, 1,8ºC, 2.1ºC and 2.8ºC by 2100 in RCPs 3PD, 4.5, 6.0, and 8.5 respectively (see Supplementary Figure S45 for spatial patterns of warming in RCP4.5). This can be compared to 0.6ºC and 2.0ºC warming in the top 100m in CMIP5 for RCPs 2.6 and 8.5, with the apparent bias towards greater warming in cGEnIE reflecting the

narrower surface layer (80.8m) versus the CMIP5 assessment. For baselines, cGEnIE's (BIO+FPR) preindustrial surface air temperature (SAT) global baseline (1850-1900) is ~12.5ºC and the preindustrial sea surface temperature (SST) global baseline is ~18.8ºC, both of which also lie within the CMIP5 range (SAT towards the lower end, SST in the higher end) (see Supplementary Figure S46 for spatial patterns of preindustrial warmth in RCP4.5).

4.2. Biological Pump Strength

[Table 2]

Our results show that the biological pump weakens under almost all scenarios and configurations, but adding TDR and trait-based plankton ecology with flexible stoichiometry has strong and opposite impacts on relative biological pump strength.

[Figure 2]

Under the default cGEnIE configuration (BIO+FPR) anthropogenic climate change results in an overall weakening of the global biological pump, with global POC flux falling below preindustrial by 2100 CE by ~6.2% under RCP4.5 and ~9.5% under RCP8.5 (Figure 2; Table 2; Supplementary Figure S47). This is in line with past projections of a 7.2% decline in surface POC export under SRES A2 (warming levels between RCPs 6.0 and 8.5) during the 21st century in a EMIC with an NPZD biogeochemistry module (Taucher and Oschlies, 2011), and a selection of CMIP5 ESMs declining by between ~6 and ~19% under RCP8.5 during the 21st century predominantly in the lower latitudes (Bopp et al., 2013; Cabré et al., 2015). In cGEnIE this is primarily driven by stratification resulting in reduced surface nutrient concentrations and decreased primary production in high-productivity low-latitude waters (Figure 3, left) in line with previous model results (Bopp et al., 2005; Ciais et al., 2013; Crichton et al., 2021; Riebesell et al., 2009; Sarmiento et al., 2004). In contrast, there is an increase in production in high-latitude waters, where the mixed layer is already so much deeper than cGEnIE's surface layer (mostly >>100m, versus cGEnIE's ~81m surface layer; Supplementary Figure S48) that stratification actually increases productivity by more effectively confining nutrients within cGEnIE's surface layer. This partially matches theoretical expectations in which stratification drives increased polar productivity by confining phytoplankton within the euphotic zone (Riebesell et al., 2009), but the mechanism driving this effect in cGEnIE is different as plankton are confined to the surface layer.

[Figure 3]

Adding TDR (BIO+TDR) leads to a substantially different result than the default cGEnIE configuration, with a far smaller biological pump weakening of only ~0.3% under RCP4.5 and ~2.1% under RCP8.5 by 2100 CE, and eventually a net

strengthening after 2100 (Figure 2). This occurs in the model because adding TDR results in an initial decrease in biological pump strength with warming as more POC is remineralised within the surface layer, which also leads to a shallower remineralisation depth and an increase in nutrient recycling and regenerated production in the surface layer. While an increase in nutrient recycling within the surface layer can lead to an increase in production by reducing nutrient loss, it does not directly lead to an increase in export as well as it is the reduction in export driving the increase in production. Only a new allochthonous source of nutrients would allow sustained increases in both production and export (Dugdale and Goering, 1967; Laws, 1991; Laws et al., 2000). However, a secondary effect of the remineralisation depth shoaling is to increase PO_4 concentrations in the layer below the productive surface (cGEnIE layers 2-3, ~81-283m) from remineralisation that would otherwise have occurred deeper in intermediate waters (Supplementary Figure S49). This in turn leads to increased allochthonous PO_4 input to the surface layer through mixing, which is sufficient to lead to an elevated baseline in new production and POC export in warmer lower-latitude waters (Figure 4a) and stimulate a relative increase in POC export with further warming. This result is consistent with previous modelling, which has shown that shoaling of the remineralisation depth in a common biogeochemical model leads to increased POC export (Kwon et al., 2009), and that including TDR in an EMIC resulted in increased Net Primary Production and a marginally smaller decrease in POC export under RCP8.5 (Taucher and Oschlies, 2011). A recent update to cGEnIE's TDR scheme (Crichton et al., 2021) also found a similar result, with historical warming resulting in a ~0.3% decline in POC export with TDR activated versus ~2.9% without. In contrast, in higher latitudes including TDR leads to a lower baseline POC export than with FPR (Figure 4a), as colder waters result in a deep remineralisation depth and less PO_4 returned to the surface layer.

[Figure 4]

Activating ecoGEnIE (ECO+FPR) instead of TDR results in a greater weakening of the biological pump than in BIO+FPR, with global POC flux falling by ~10.2% by 2100 CE under RCP4.5 and ~15.4% under RCP8.5 (Figure 2). Adding ECOGEM allows an overall decrease in average plankton size in response to climate change (Supplementary Figure S50), as warming and stratification leads to oligotrophication in lower latitude waters which favours smaller plankton size classes, and is in line with previous observational and modelling studies (Finkel et al., 2010; Riebesell et al., 2009). Smaller taxa produce more DOM than POM (Finkel et al., 2010) and so the shift to smaller plankton classes in warmer regions decreases overall POC and PIC export (Figure 4b), while the shift to smaller taxa lower in the food chain extends the number of trophic levels and so reduces the efficiency and productivity of the whole ecosystem (Supplementary Figure S51) (Riebesell et al., 2009). This decline is sufficient to counteract the negative feedback of the shift to smaller particles increasing surface nutrient recycling due to shallower remineralisation (Leung et al., 2021). Activating ECOGEM also enables flexible stoichiometry, but the effect of this is difficult to disentangle from that of multiple size classes as well. However, some patterns and trends can be seen. The preindustrial POM export C:P ratio lies above the standard Redfield ratio of 106:1 across most of the ocean outside the Southern Ocean, reaching ~200:1 in equatorial upwelling regions and the global mean closely matching recent observations

of 163:1 (Supplementary Figure S52) (Martiny et al., 2014). By 2100 CE this ratio increases across almost the entire ocean, especially along the Antarctic Polar Front and in the Arctic Ocean (Supplementary Figure S53). This indicates that the amount of carbon exported for every unit of phosphorus increases with warming in response to stratification, reducing surface phosphorus loss and so partly ameliorating the decline in carbon export.

Without stratification and nutrient restriction, higher temperatures in a previous ecoGEnIE study resulted in an increase in export production and mean cell size despite an overall decrease in biomass (Wilson et al., 2018). Although the increase in phytoplankton nutrient usage (which is temperature-dependent in ecoGEnIE) boosted small phytoplankton production in their study, this increase was assimilated by zooplankton grazing (which is also temperature-dependent). This allowed larger phytoplankton to compete against small phytoplankton with higher nutrient affinities, and resulted in increased particulate export from larger phytoplankton and inefficient zooplankton feeding despite lower overall ecosystem biomass (Ward et al., 2014). When nutrient fluxes were increased without higher temperatures, increases in small phytoplankton biomass were again limited by zooplankton grazing and made larger phytoplankton more competitive, but unlike warming alone higher nutrient fluxes facilitated both elevated total ecosystem production and export. In our ecoGEnIE results though higher temperatures are accompanied by both stratification and reduced nutrient flux in low-latitudes, resulting in an overall shift to smaller phytoplankton dominance despite warming allowing greater phytoplankton nutrient usage and grazing. The consequent reduction in grazing and large phytoplankton abundance in turn accentuates the decline in POC export from declining low latitude ecosystem biomass, leading to a greater decline in POC export than BIO+FPR and BIO+TDR.

In contrast to low-latitudes, in most high-latitude waters biomass increases while mean cell size and export decline (Supplementary Figures S50, S51 & S54), and along the Antarctic Polar Front biomass decreases, mean cell size is stable or increases, and POC export increases. The latter is because warming in nutrient-rich upwelling regions allows for increased zooplankton and larger phytoplankton abundance (Supplementary Figures S55-60) and therefore leads to restrained total biomass due to grazing coupled with increased export. In non-upwelling polar regions such as the western Arctic where nutrients are limited but unlike in low-latitudes warming-induced stratification does not restrict nutrient flux further, warming preferentially boosts smaller phytoplankton (6µm vs. 19µm) which along with a commensurate decline in dependent zooplankton (19µm) and top-down grazing pressure leads to increased overall biomass but lower export. In the eastern Arctic this process is not as apparent due to the interference of Atlantic meridional overturning slowdown resulting in a moderate reduction in formerly elevated nutrient availability. This leads to a reduction in medium relative to small phytoplankton classes (19µm vs. 1.9 & 6µm) and a commensurate shift to smaller zooplankton classes (6 & 19µm vs. 60µm), and therefore relatively stable biomass and mean cell size coupled with reduced export

Adding both trait-based plankton ecology and TDR (ECO+TDR) produces a complex result, with the weakening effect of adding ECO on the biological pump partly counteracting the strengthening effect of adding TDR. The overall effect is a

moderate net weakening of the biological pump by ~7.9% by 2100 CE under RCP4.5 and ~12.3% under RCP8.5 (Figure 2), as decreasing plankton size and POC export in lower latitude waters due to adding ECO reduces the capacity for nutrient recycling to increase as a result of adding TDR (Figure 4c). The combined effect of ECO+TDR relative to BIO+FPR in this model is therefore an additional ~1.4% weakening of the biological pump by 2100 CE relative to preindustrial across the RCPs (Figure 3, right), resulting in ~9-11 Pg less POC being exported by the biological pump in this model by 2100. In all configurations and scenarios the changes in the biological pump continue past 2100 CE, and in many cases only begin to stabilise after several hundred years (Figure 2).

Using the published or default calibrations for each configuration instead of our recalibrations results in the same overall pattern of TDR ameliorating and ECO amplifying the biological pump weakening with warming, but with a reduced weakening for ECO+FPR and ECO+TDR, greater long-term strengthening for BIO+TDR, and a smaller rather than greater net weakening in uncalibrated ECO+TDR than for BIO+FPR (Supplementary Figure S61). However, these calibrations have substantially different baseline biological pumps, with higher POC export in the uncalibrated configurations with TDR and/or ECO. High production and export leads to differing initial ecosystem structure and therefore amplified effects on remineralisation when POC export changes with warming, which acts as a confounding factor when comparing their responses.

4.3. Ocean Carbon Sink Capacity

It has sometimes been implied in previous discussions of empirical and model results that a decrease in biological pump strength directly leads to a corresponding decrease in the ocean carbon sink capacity, as less POC is exported from the surface to deep ocean and so more CO_2 remains in surface waters and therefore the atmosphere (Boscolo-Galazzo et al., 2018; John et al., 2014a; Olivarez Lyle and Lyle, 2006; Steffen et al., 2018). However, reduced POC export affects many other processes, which results in a nonlinear relation between biological pump strength and the ocean carbon sink capacity that can lead to counter-intuitive outcomes (Gnanadesikan and Marinov, 2008; Kwon et al., 2009).

[Figure 5]

In our simulations, the relative strengthening of the biological pump when TDR is included actually leads to a net decrease in the ocean carbon sink capacity by 2100 CE (Table 2, Figure 5). Conversely, the relative weakening of the biological pump with ECOGEM activated instead (ECO+FPR) is associated with a net increase in the ocean carbon sink capacity. Combining both ECOGEM and TDR (ECO+TDR) results in a smaller overall relative weakening of the biological pump compared to default, and a marginal net decrease in the ocean carbon sink capacity of ~0.4 PgC under RCP4.5 (~2.3 PgC under RCP8.5) by 2100 CE (Table 2). Beyond the 21st century though, ECO+TDR eventually results in a net increase in ocean carbon sink

capacity from the 22nd century onwards (Figure 5). Including trait-based ecology using size classes therefore largely but not entirely offsets the impact on the ocean carbon sink of also including TDR in this model during the 21st century, and entirely offsets the TDR-induced sink decline after that. The model thus suggests that ecological dynamics increases the resilience of plankton ecosystem functioning against the pressures of climate change.

A decrease in particulate export does not automatically result in a decrease in the ocean carbon sink capacity in this model as a result of interactions with carbonate chemistry and ocean acidification. Adding TDR results in greater production of both POC and PIC relative to BIO+FPR in non-polar regions in response to warming, as described in the Section 4.2. Increased photosynthesis and $CaCO_3$ formation results in an initial net decrease in surface DIC and ALK, which through DIC speciation leads to a decrease in the concentration of dissolved carbonate ($[CO_3]$), an increase in the concentration of surface dissolved CO_2 ($[CO_2]$), and decreased pH and carbonate saturation state (Ω) (as theoretically described by Zeebe and Wolf-Gladrow, 2001). This increases the partial pressure of CO_2 in surface waters (pCO_2), therefore reducing the capacity for additional CO_2 to dissolve from the atmosphere into the ocean. This effect on the air-to-sea CO_2 flux gradually limits the total DIC content for the whole ocean and therefore the ocean carbon sink as a whole (see explanatory schematic in Supplementary Figure S62). Ocean acidification also concurrently increases surface pCO_2 and decreases Ω and PIC production (Supplementary Figure S63), and so adding TDR results in a synergistic interaction with ocean acidification. Conversely, as shown in Section 4.2 adding ECOGEM reduces total ecosystem POC and PIC production with warming as a result of the shift to smaller plankton taxa, leading to higher surface DIC and ALK, increased surface $[CO_3]$ and Ω, decreased surface $[CO_2]$ and pCO_2, and therefore increased air-to-sea CO_2 flux and total ocean DIC in the long-term. Introducing ECOGEM and the resultant oligotrophication-induced plankton size shift therefore slightly counters the ocean acidification trend.

It is possible that the small differences in surface carbonate chemistry between the different model configurations have a confounding effect on our carbon sink results. BIO+TDR has ~7.5% lower baseline $[CO_3]$ than BIO+FPR (Supplementary Table S1), which as discussed in Section 3.3 somewhat reduces carbonate buffering and so could explain a proportion of the simulated carbon sink weakening through a reduced solubility pump. Using the published or default calibrations of each configuration instead (Supplementary Figure S64) reduces the long-term sink strengthening effect by ECO and enhances sink weakening by TDR relative to the recalibrated configurations, which results in a sustained net sink weakening with ECO+TDR relative to the recalibrations. However, these original calibrations have substantially different baseline biological pumps and carbonate chemistry, which act as confounding factors in their response. POC production and export is higher and more resilient against warming in the original TDR and ECO calibrations (Supplementary Table S1 and Figure S64), and therefore has a reduced impact on surface carbonate chemistry. In the ECO configurations $[CO_3]$ is also much weaker (~70-80 vs, ~106 $\mu mol\ kg^{-1}$ in BIO+FPR) and $[CO_2]$ much higher (~40-50 vs. 24 $\mu mol\ kg^{-1}$ in BIO+FPR) than in the recalibrations, resulting in substantially weaker carbonate buffering in the uncalibrated configurations. Both higher and lower $[CO_3]$ in the original BIO+TDR and ECO calibrations respectively are also associated with reduced carbon sink capacity relative to the

recalibrations across all configurations, while in the recalibrated configurations ECO+FPR shows an increase in carbon sink capacity despite lower [CO_3] than ECO+TDR. Together this indicates that [CO_3] has a relatively minor impact on the sign and magnitude of our carbon sink results.

5. Discussion

These results clearly illustrate the importance of incorporating multiple dimensions of ecological complexity within Earth system models in order to capture the impact of nonlinear climate-biosphere feedbacks, biodiversity, and ecological resilience on the future dynamics of carbon sinks. However, although the introduction of either TDR or ECO leads to substantially different changes in POC export in response to warming, the impact on the overall ocean carbon sink is less pronounced. Our ecoGEnIE experiments simulate a modest decline in the ocean carbon sink capacity of around ~6 PgC (~0.06 $PgCy^{-1}$) during the 21st Century under an RCP8.5 scenario when accounting for TDR. This can be compared to a previous estimate of a ~18 PgC (~0.18 $PgCy^{-1}$) decline in ocean carbon sink capacity by 2100 in response to RCP8.5 made using a simpler NPZD-based ecosystem representation that differentiated silicifying plankton (Segschneider and Bendtsen, 2013), and to the 2018 ocean carbon sink uptake rate of 2.6±0.6 $PgCy^{-1}$ (Friedlingstein et al., 2019). This decline is partially countered when greater ecological complexity and flexible stoichiometry is introduced as well, with a shift to smaller plankton classes in response to oligotrophication leading to an ocean carbon sink reduction of only ~2.3 PgC. Other processes that are not resolved in this configuration of ecoGEnIE could also substantially affect the biological pump though, such as ballasting, calcifier-silicifier trade-offs, nitrogen cycle and stoichiometry-acidification feedbacks (Buchanan et al., 2019; Dutkiewicz et al., 2015; Landolfi et al., 2017; Riebesell et al., 2007; Somes et al., 2016; Tagliabue et al., 2011), deep chlorophyll maxima, and on longer timescales redox-dependent feedbacks (Niemeyer et al., 2017; Watson, 2016). Limited physical resolution can also have significant impacts on biogeochemistry (Sinha et al., 2010), and so also limits our results Further work is required to assess the impact of these features on our estimates.

Few of the ESMs used in CMIP5 sufficiently resolve marine ecology, instead relying on simple plankton ecosystems that are often highly parameterised with minimal or non-existent ecological and metabolic dynamics (Table 1). This reduces computational expense and so allows higher resolution of important physical processes, but comes at the price of poorly resolving known biogeochemical and ecological feedbacks that can substantially affect carbon partitioning (Anderson, 2005; Ward et al., 2018). To date, gains in computational power have largely been allocated to improved resolution and physical process representation, while despite recent progress biogeochemical parameters have remained too poorly constrained to allow greater biogeochemical complexity in high resolution ESMs. However, the development of trait-based ecological models could enable ESMs to include more complex marine biogeochemical modules without compromising the high resolution representation of physical processes. An approach that focuses on functional traits and generic ecosystem rules potentially reduces the need for taxonomic-specific parameterisations and also allows better representation of allometric effects.

Development of biogeochemical models with higher physical resolution would also allow more accurate representation of fine-scale biogeochemical processes such as the interaction of stratification, the nutricline, and deep chlorophyll maxima in oligotrophic regions (Richardson and Bendtsen, 2017, 2019), issues raised in this study that have not been possible to explore. EMICs with lower physical resolution can more readily incorporate ecological complexity though, and remain a crucial tool for further exploring these feedbacks in the interim (Chien et al., 2020; Frants et al., 2016; Kriest, 2017; Kriest et al., 2020; Niemeyer et al., 2019; Sauerland et al., 2019; Schartau et al., 2017; Ward et al., 2018; Wilson et al., 2018; Yao et al., 2019).

In this study we focus on the dominant soft-tissue biological pump, but the variable response of plankton classes with different shell types to climate change and ocean acidification also has an impact on the biological pump. For instance, silicifiers with opal-based shells such as diatoms thrive in nutrient-rich waters. Segschneider and Bendtsen (2013) found that the increased nutrient recycling when TDR was introduced in their model initially drives an increase in diatom production and opal export in response to climate change. In their model, this soon leads to silicate-depleted surface waters and suppressed diatom production, allowing a subsequent increase in calcifying plankton and PIC export instead. This has the effect of reducing surface alkalinity and increasing surface pCO_2, which drives a substantial proportion of the large ocean carbon sink reduction in their analysis. Despite the likely importance of this 'hard-shell' mechanism, ecoGEnIE does not currently allow independent representation of calcifiers and does not represent silicifiers at all, and so the potential impact of this mechanism is not resolved by our results. However, the model of Segschneider and Bendtsen (2013) does not feature size classes or flexible stoichiometry, which we have shown is important for determining the soft-tissue biological pump response. In order to fully compare our results it will be necessary to repeat our simulations with the silicifier-enabled ECOGEM currently under development. Together, resolving plankton size classes, TDR, flexible stoichiometry, and separate silicifier and calcifier functional types will allow the response of the marine biological pump to climate change to be more fully diagnosed.

Further development will also allow the potential impact of ballasting to be assessed. Using a different EMIC, (Kvale et al., 2015, 2019) found that adding ballasting alongside calcifier functional types mitigated the biological pump response to ocean warming by facilitating increased calcifier production and therefore increasing nutrient export from the surface. In contrast, activating ballasting in ecoGEnIE without separating out a competitive calcifier functional type would likely result in greater surface layer remineralisation in scenarios with reduced PIC production. However, empirical observations have suggested that the ballasting effect on the ocean carbon sink is weaker than has been hypothesised (Wilson et al., 2012).

6. Conclusions

The response of the biological pump to climate change is important for projecting climate feedbacks and the future behaviour of the ocean carbon sink, but many of the most influential Earth system models fail to incorporate sufficient metabolic or

ecological complexity for this to be fully resolved. In this study, we have investigated the impact of integrating temperature-dependent remineralisation, size-based biodiversity, and flexible nutrient usage on the biological pump and ocean carbon sink in response to climate change. As expected, we found that adding temperature-dependent remineralisation to an Earth system model of intermediate complexity (ecoGEnIE) results in a greater weakening of the ocean carbon sink as a result of climate change. However, this actually results from a relative strengthening of the biological pump itself as a result of shallower nutrient remineralisation, contrary to the common expectation that the direct effect of warming further amplifies a weakening of the biological pump. Conversely, adding trait-based ecosystem dynamics instead results in an even weaker biological pump as a result of oligotrophication favouring smaller plankton, and in turn a larger ocean carbon sink. Finally, combining both of these features results in a smaller relative weakening of the biological pump and a modest reduction in the ocean carbon sink capacity.

Together, this implies that the biological pump positive feedback on climate change may be larger than CMIP5 models project, but is potentially less than some more recent model projections (Segschneider and Bendtsen, 2013; Steffen et al., 2018). This study has primarily focused on the allometric aspects of dominant soft-tissue components of the biological pump, and the results clearly illustrate the substantial degree to which ecological dynamics and biodiversity can modulate the strength of climate-biosphere feedbacks. These complex relations require further analyses and validation, but at present comparison of model studies is a challenge because today's ESMs take such different approaches and simplifications. Trait-based ecological modules that go beyond simple biogeochemical traits could in future enable ESMs to include more ecological complexity without compromising the high resolution representation of physical processes, and allow feedbacks such as the marine biological pump to be more fully resolved in future.

Author Contributions

DIAM, SEC, & KR conceived of the study; DIAM designed the study, configured and ran the model, and performed the analyses; DIAM wrote the paper with input from SEC, KR, & JR.

Data availability

cGEnIE.muffin is available for download from https://github.com/derpycode/cgenie.muffin, and a manual detailing code installation, model configuration, and extensive tutorials is available from https://github.com/derpycode/muffindoc. Modern observational data for model-data comparison are available from http://www.seao2.info/mymuffin.html. CO_2 emission scenarios for forcing the model are available from http://www.pik-potsdam.de/~mmalte/rcps/ (Meinshausen et al., 2011).

Conflicts of Interest

The authors declare that they have no conflict of interest

Acknowledgements

This work was supported by the European Research Council Advanced Investigator project "Earth Resilience in the Anthropocene" ERA (ERC-2016-ADG-743080) and a core grant to Stockholm Resilience Centre by Mistra. We thank Andy Ridgwell and Ben Ward for discussions on using ecoGEnIE, and Toby Tyrrell for discussions on variable stoichiometry.

References

Anderson, T. R.: Plankton functional type modelling: Running before we can walk?, J. Plankton Res., 27(11), 1073–1081, doi:10.1093/plankt/fbi076, 2005.

Armstrong, R. A., Lee, C., Hedges, J. I., Honjo, S. and Wakeham, S. G.: A new, mechanistic model for organic carbon fluxes in the ocean based on the quantitative association of POC with ballast minerals, Deep Sea Res. Part II Top. Stud. Oceanogr., 49(1–3), 219–236, doi:10.1016/S0967-0645(01)00101-1, 2001.

Arora, V. K., Boer, G. J., Friedlingstein, P., Eby, M., Jones, C. D., Christian, J. R., Bonan, G., Bopp, L., Brovkin, V., Cadule, P., Hajima, T., Ilyina, T., Lindsay, K., Tjiputra, J. F. and Wu, T.: Carbon-concentration and carbon-climate feedbacks in CMIP5 earth system models, J. Clim., 26(15), 5289–5314, doi:10.1175/JCLI-D-12-00494.1, 2013.

Aumont, O., Maier-Reimer, E., Blain, S. and Monfray, P.: An ecosystem model of the global ocean including Fe, Si, P colimitations, Global Biogeochem. Cycles, 17(2), n/a-n/a, doi:10.1029/2001GB001745, 2003.

Beaugrand, G., Edwards, M. and Legendre, L.: Marine biodiversity, ecosystem functioning, and carbon cycles, Proc. Natl. Acad. Sci. U. S. A., 107(22), 10120–10124, doi:10.1073/pnas.0913855107, 2010.

Bendtsen, J., Hilligsøe, K. M., Hansen, J. L. S. and Richardson, K.: Analysis of remineralisation, lability, temperature sensitivity and structural composition of organic matter from the upper ocean, Prog. Oceanogr., 130(October 2014), 125–145, doi:10.1016/j.pocean.2014.10.009, 2015.

Bopp, L., Aumont, O., Cadule, P., Alvain, S. and Gehlen, M.: Response of diatoms distribution to global warming and potential implications: A global model study, Geophys. Res. Lett., 32(19), 1–4, doi:10.1029/2005GL023653, 2005.

Bopp, L., Resplandy, L., Orr, J. C., Doney, S. C., Dunne, J. P., Gehlen, M., Halloran, P., Heinze, C., Ilyina, T., Séférian, R., Tjiputra, J. and Vichi, M.: Multiple stressors of ocean ecosystems in the 21st century: projections with CMIP5 models, Biogeosciences, 10(10), 6225–6245, doi:10.5194/bg-10-6225-2013, 2013.

Boscolo-Galazzo, F., Crichton, K. A., Barker, S. and Pearson, P. N.: Temperature dependency of metabolic rates in the upper ocean: A positive feedback to global climate change?, Glob. Planet. Change, 170(March), 201–212, doi:10.1016/j.gloplacha.2018.08.017, 2018.

Broecker, W. S. and Peng, T.-H.: Tracers in the sea, Lamont-Doherty Geological Observatory, Palisades, New York., 1982.

Bruggeman, J. and Kooijman, S. A. L. M.: A biodiversity-inspired approach to aquatic ecosystem modeling, Limnol. Oceanogr., 52(4), 1533–1544, doi:10.4319/lo.2007.52.4.1533, 2007.

Buchanan, P. J., Chase, Z., Matear, R. J., Phipps, S. J. and Bindoff, N. L.: Marine nitrogen fixers mediate a low latitude pathway for atmospheric CO2 drawdown, Nat. Commun., 10(1), 1–10, doi:10.1038/s41467-019-12549-z, 2019.

Cabré, A., Marinov, I. and Leung, S.: Consistent global responses of marine ecosystems to future climate change across the IPCC AR5 earth system models, Clim. Dyn., 45(5–6), 1253–1280, doi:10.1007/s00382-014-2374-3, 2015.

Chien, C. Te, Pahlow, M., Schartau, M. and Oschlies, A.: Optimality-based non-Redfield plankton-ecosystem model (OPEM v1.1) in UVic-ESCM 2.9 - Part 2: Sensitivity analysis and model calibration, Geosci. Model Dev., 13(10), 4691–4712, doi:10.5194/gmd-13-4691-2020, 2020.

Ciais, P., Sabine, C., Bala, G., Bopp, L., Brovkin, V., Canadell, J., Chhabra, A., DeFries, R., Galloway, J., Heimann, M., Jones, C., Quéré, C. Le, Myneni, R. B., Piao, S. and Thornton, P.: Carbon and Other Biogeochemical Cycles, in Climate Change 2013 - The Physical Science Basis, edited by Intergovernmental Panel on Climate Change, pp. 465–570, Cambridge University Press, Cambridge., 2013.

Claussen, M., Mysak, L., Weaver, A., Crucifix, M., Fichefet, T., Loutre, M. F., Weber, S., Alcamo, J., Alexeev, V., Berger, A., Calov, R., Ganopolski, A., Goosse, H., Lohmann, G., Lunkeit, F., Mokhov, I., Petoukhov, V., Stone, P. and Wang, Z.: Earth system models of intermediate complexity: Closing the gap in the spectrum of climate system models, Clim. Dyn., 18(7), 579–586, doi:10.1007/s00382-001-0200-1, 2002.

Collins, M., Knutti, R., Arblaster, J., Dufresne, J.-L., Fichefet, T., Friedlingstein, P., Gao, X., Gutowski, W. J., Johns, T., Krinner, G., Shongwe, M., Tebaldi, C., Weaver, A. J. and Wehner, M.: Long-term Climate Change: Projections, Commitments and Irreversibility, in Climate Change 2013: The Physical Science Basis. Contribution of Working Group I to the Fifth Assessment Report of the Intergovernmental Panel on Climate Change, edited by V. B. and P. M. M. Stocker, T.F., D. Qin, G.-K. Plattner, M. Tignor, S.K. Allen, J. Boschung, A. Nauels, Y. Xia, Cambridge University Press, Cambridge, UK; New York, USA., 2013.

Crichton, K. A., Wilson, J. D., Ridgwell, A. and Pearson, P. N.: Calibration of temperature-dependent ocean microbial processes in the cGENIE.muffin (v0.9.13) Earth system model, Geosci. Model Dev., 14(1), 125–149, doi:10.5194/gmd-14-125-2021, 2021.

Doney, S. C., Busch, D. S., Cooley, S. R. and Kroeker, K. J.: The Impacts of Ocean Acidification on Marine Ecosystems and Reliant Human Communities, Annu. Rev. Environ. Resour., 45(1), 1–30, doi:10.1146/annurev-environ-012320-083019, 2020.

Dugdale, R. C. and Goering, J. J.: Uptake of New and Regenerated Forms of Nitrogen in Primary Productivity, Limnol. Oceanogr., 12(2), 196–206, doi:10.4319/lo.1967.12.2.0196, 1967.

Dunne, J. P., Sarmiento, J. L. and Gnanadesikan, A.: A synthesis of global particle export from the surface ocean and cycling through the ocean interior and on the seafloor, Global Biogeochem. Cycles, 21(4), 1–16, doi:10.1029/2006GB002907, 2007.

Dutkiewicz, S., Morris, J. J., Follows, M. J., Scott, J., Levitan, O., Dyhrman, S. T. and Berman-Frank, I.: Impact of ocean acidification on the structure of future phytoplankton communities, Nat. Clim. Chang., 5(11), 1002–1006, doi:10.1038/nclimate2722, 2015.

Edwards, N. R. and Marsh, R.: Uncertainties due to transport-parameter sensitivity in an efficient 3-D ocean-climate model, Clim. Dyn., 24(4), 415–433, doi:10.1007/s00382-004-0508-8, 2005.

Eppley, R. W.: Fishery Bulletin Vol70 No4 1972.Pdf, Fish. Bull., 70(4), 1063–1085, 1972.

Fakhraee, M., Planavsky, N. J. and Reinhard, C. T.: The role of environmental factors in the long-term evolution of the marine biological pump, Nat. Geosci., 13(12), 812–816, doi:10.1038/s41561-020-00660-6, 2020.

Finkel, Z. V., Beardall, J., Flynn, K. J., Quigg, A., Rees, T. A. V. and Raven, J. A.: Phytoplankton in a changing world: cell size and elemental stoichiometry, J. Plankton Res., 32(1), 119–137, doi:10.1093/plankt/fbp098, 2010.

Follows, M. J., Dutkiewicz, S., Grant, S. and Chisholm, S. W.: Emergent biogeography of microbial communities in a model ocean, Science, 315(5820), 1843–1846, doi:10.1126/science.1138544, 2007.

Frants, M., Holzer, M., DeVries, T. and Matear, R.: Constraints on the global marine iron cycle from a simple inverse model, J. Geophys. Res. Biogeosciences, 121(1), 28–51, doi:10.1002/2015JG003111, 2016.

Friedlingstein, P., Jones, M. W., O'Sullivan, M., Andrew, R. M., Hauck, J., Peters, G. P., Peters, W., Pongratz, J., Sitch, S., Le Quéré, C., DBakker, O. C. E., Canadell1, J. G., Ciais1, P., Jackson, R. B., Anthoni1, P., Barbero, L., Bastos, A., Bastrikov, V., Becker, M., Bopp, L., Buitenhuis, E., Chandra, N., Chevallier, F., Chini, L. P., Currie, K. I., Feely, R. A., Gehlen, M., Gilfillan, D., Gkritzalis, T., Goll, D. S., Gruber, N., Gutekunst, S., Harris, I., Haverd, V., Houghton, R. A., Hurtt, G., Ilyina, T., Jain, A. K., Joetzjer, E., Kaplan, J. O., Kato, E., Goldewijk, K. K., Korsbakken, J. I., Landschützer, P., Lauvset, S. K., Lefèvre, N., Lenton, A., Lienert, S., Lombardozzi, D., Marland, G., McGuire, P. C., Melton, J. R., Metzl, N., Munro, D. R., Nabel, J. E. M. S., Nakaoka, S. I., Neill, C., Omar, A. M., Ono, T., Peregon, A., Pierrot, D., Poulter, B., Rehder, G., Resplandy, L., Robertson, E., Rödenbeck, C., Séférian, R., Schwinger, J., Smith, N., Tans, P. P., Tian, H., Tilbrook, B., Tubiello, F. N., Van Der Werf, G. R., Wiltshire, A. J. and Zaehle, S.: Global carbon budget 2019, Earth Syst. Sci. Data, 11(4), 1783–1838, doi:10.5194/essd-11-1783-2019, 2019.

Friedrichs, M. A. M., Dusenberry, J. A., Anderson, L. A., Armstrong, R. A., Chai, F., Christian, J. R., Doney, S. C., Dunne, J., Fujii, M., Hood, R., McGillicuddy, D. J., Moore, J. K., Schartau, M., Spitz, Y. H. and Wiggert, J. D.: Assessment of skill and portability in regional marine biogeochemical models: Role of multiple planktonic groups, J. Geophys. Res. Ocean., 112(8), 1–22, doi:10.1029/2006JC003852, 2007.

Galbraith, E. D. and Martiny, A. C.: A simple nutrient-dependence mechanism for predicting the stoichiometry of marine ecosystems, Proc. Natl. Acad. Sci., 112(27), 8199–8204, doi:10.1073/pnas.1423917112, 2015.

Galbraith, E. D., Dunne, J. P., Gnanadesikan, A., Slater, R. D., Sarmiento, J. L., Dufour, C. O., de Souza, G. F., Bianchi, D., Claret, M., Rodgers, K. B. and Marvasti, S. S.: Complex functionality with minimal computation: Promise and pitfalls of reduced-tracer ocean biogeochemistry models, J. Adv. Model. Earth Syst., 7(4), 2012–2028, doi:10.1002/2015MS000463, 2015.

Gibbs, S. J., Bown, P. R., Ridgwell, A., Young, J. R., Poulton, A. J. and O'Dea, S. A.: Ocean warming, not acidification, controlled coccolithophore response during past greenhouse climate change, Geology, 44(1), 59–62, doi:10.1130/G37273.1, 2016.

Gnanadesikan, A. and Marinov, I.: Export is not enough: Nutrient cycling and carbon sequestration, Mar. Ecol. Prog. Ser., 364, 289–294, doi:10.3354/meps07550, 2008.

Gruber, N., Clement, D., Carter, B. R., Feely, R. A., van Heuven, S., Hoppema, M., Ishii, M., Key, R. M., Kozyr, A., Lauvset, S. K., Lo Monaco, C., Mathis, J. T., Murata, A., Olsen, A., Perez, F. F., Sabine, C. L., Tanhua, T. and Wanninkhof, R.: The oceanic sink for anthropogenic CO2 from 1994 to 2007, Science, 363(6432), 1193–1199, doi:10.1126/science.aau5153, 2019.

Guidi, L., Stemmann, L., Jackson, G. A., Ibanez, F., Claustre, H., Legendre, L., Picheral, M. and Gorsky, G.: Effects of phytoplankton community on production, size and export of large aggregates: A world-ocean analysis, Limnol. Oceanogr., 54(6), 1951–1963, doi:10.4319/lo.2009.54.6.1951, 2009.

Harfoot, M. B. J., Newbold, T., Tittensor, D. P., Emmott, S., Hutton, J., Lyutsarev, V., Smith, M. J., Scharlemann, J. P. W. and Purves, D. W.: Emergent Global Patterns of Ecosystem Structure and Function from a Mechanistic General Ecosystem Model, edited by M. Loreau, PLoS Biol., 12(4), e1001841, doi:10.1371/journal.pbio.1001841, 2014.

Henson, S. A., Sanders, R., Madsen, E., Morris, P. J., Le Moigne, F. and Quartly, G. D.: A reduced estimate of the strength of the ocean's biological carbon pump, Geophys. Res. Lett., 38(4), 10–14, doi:10.1029/2011GL046735, 2011.

Henson, S. A., Sanders, R. and Madsen, E.: Global patterns in efficiency of particulate organic carbon export and transfer to the deep ocean, Global Biogeochem. Cycles, 26(1), n/a-n/a, doi:10.1029/2011GB004099, 2012.

Hoppe, H. G., Gocke, K., Koppe, R. and Begler, C.: Bacterial growth and primary production along a north-south transect of the Atlantic Ocean, Nature, 416(6877), 168–171, doi:10.1038/416168a, 2002.

John, E. H., Wilson, J. D., Pearson, P. N. and Ridgwell, A.: Temperature-dependent remineralization and carbon cycling in the warm Eocene oceans, Palaeogeogr. Palaeoclimatol. Palaeoecol., 413, 158–166, doi:10.1016/j.palaeo.2014.05.019, 2014a.

John, E. H., Wilson, J. D., Pearson, P. N. and Ridgwell, A.: Temperature-dependent remineralization and carbon cycling in the warm Eocene oceans, Palaeogeogr. Palaeoclimatol. Palaeoecol., 413, 158–166, doi:10.1016/j.palaeo.2014.05.019, 2014b.

Keeling, R. F., Körtzinger, A. and Gruber, N.: Ocean Deoxygenation in a Warming World, Ann. Rev. Mar. Sci., 2(1), 199–229, doi:10.1146/annurev.marine.010908.163855, 2010.

Klaas, C. and Archer, D. E.: Association of sinking organic matter with various types of mineral ballast in the deep sea: Implications for the rain ratio, Global Biogeochem. Cycles, 16(4), 63-1-63–14, doi:10.1029/2001gb001765, 2002.

Kriest, I.: Calibration of a simple and a complex model of global marine biogeochemistry, Biogeosciences Discuss., 1–28, doi:10.5194/bg-2017-71, 2017.

Kriest, I., Kähler, P., Koeve, W., Kvale, K., Sauerland, V. and Oschlies, A.: One size fits all? Calibrating an ocean biogeochemistry model for different circulations, Biogeosciences, 17(12), 3057–3082, doi:10.5194/bg-17-3057-2020, 2020.

Kwiatkowski, L., Yool, A., Allen, J. I., Anderson, T. R., Barciela, R., Buitenhuis, E. T., Butenschön, M., Enright, C., Halloran, P. R., Le Quéré, C., De Mora, L., Racault, M. F., Sinha, B., Totterdell, I. J. and Cox, P. M.: IMarNet: An ocean biogeochemistry model intercomparison project within a common physical ocean modelling framework, Biogeosciences, 11(24), 7291–7304, doi:10.5194/bg-11-7291-2014, 2014.

Kwiatkowski, L., Aumont, O., Bopp, L. and Ciais, P.: The Impact of Variable Phytoplankton Stoichiometry on Projections of Primary Production, Food Quality, and Carbon Uptake in the Global Ocean, Global Biogeochem. Cycles, 32(4), 516–528, doi:10.1002/2017GB005799, 2018.

Kwon, E. Y., Primeau, F. and Sarmiento, J. L.: The impact of remineralization depth on the air-sea carbon balance, Nat. Geosci., 2(9), 630–635, doi:10.1038/ngeo612, 2009.

Landolfi, A., Somes, C. J., Koeve, W., Zamora, L. M. and Oschlies, A.: Oceanic nitrogen cycling and N2O flux perturbations in the Anthropocene, Global Biogeochem. Cycles, 31(8), 1236–1255, doi:10.1002/2017GB005633, 2017.

Laws, E. A.: Photosynthetic quotients, new production and net community production in the open ocean, Deep Sea Res. Part A. Oceanogr. Res. Pap., 38(1), 143–167, doi:10.1016/0198-0149(91)90059-O, 1991.

Laws, E. A., Falkowski, P. G., Smith, W. O., Ducklow, H. and McCarthy, J. J.: Temperature effects on export production in the open ocean, Global Biogeochem. Cycles, 14(4), 1231–1246, doi:10.1029/1999GB001229, 2000.

Leung, S. W., Weber, T., Cram, J. A. and Deutsch, C.: Variable particle size distributions reduce the sensitivity of global export flux to climate change, Biogeosciences, 18(1), 229–250, doi:10.5194/bg-18-229-2021, 2021.

Marsh, R., Müller, S. A., Yool, A. and Edwards, N. R.: Incorporation of the C-GOLDSTEIN efficient climate model into the GENIE framework: "eb_go_gs" configurations of GENIE, Geosci. Model Dev., 4(4), 957–992, doi:10.5194/gmd-4-957-2011, 2011.

Martin, J. H., Knauer, G. A., Karl, D. M. and Broenkow, W. W.: VERTEX: carbon cycling in the northeast Pacific, Deep Sea Res. Part A, Oceanogr. Res. Pap., 34(2), 267–285, doi:10.1016/0198-0149(87)90086-0, 1987.

Martiny, A. C., Vrugt, J. A. and Lomas, M. W.: Concentrations and ratios of particulate organic carbon, nitrogen, and phosphorus in the global ocean, Sci. Data, 1, 1–7, doi:10.1038/sdata.2014.48, 2014.

Martiny, A. C., Ma, L., Mouginot, C., Chandler, J. W. and Zinser, E. R.: Interactions between thermal acclimation, growth rate, and phylogeny influence prochlorococcus elemental stoichiometry, PLoS One, 11(12), 1–12, doi:10.1371/journal.pone.0168291, 2016.

McGill, B. J., Enquist, B. J., Weiher, E. and Westoby, M.: Rebuilding community ecology from functional traits, Trends Ecol. Evol., 21(4), 178–185, doi:10.1016/j.tree.2006.02.002, 2006.

Meinshausen, M., Smith, S. J., Calvin, K., Daniel, J. S., Kainuma, M. L. T., Lamarque, J.-F., Matsumoto, K., Montzka, S. A., Raper, S. C. B., Riahi, K., Thomson, A., Velders, G. J. M. and van Vuuren, D. P. P.: The RCP greenhouse gas concentrations and their extensions from 1765 to 2300, Clim. Change, 109(1–2), 213–241, doi:10.1007/s10584-011-0156-z, 2011.

Meyer, K. M., Ridgwell, A. and Payne, J. L.: The influence of the biological pump on ocean chemistry: Implications for long-term trends in marine redox chemistry, the global carbon cycle, and marine animal ecosystems, Geobiology, 14(3), 207–219,

doi:10.1111/gbi.12176, 2016.

Monteiro, F. M., Pancost, R. D., Ridgwell, A. and Donnadieu, Y.: Nutrients as the dominant control on the spread of anoxia and euxinia across the Cenomanian-Turonian oceanic anoxic event (OAE2): Model-data comparison, Paleoceanography, 27(4), 1–17, doi:10.1029/2012PA002351, 2012.

Moreno, A. R. and Martiny, A. C.: Ecological Stoichiometry of Ocean Plankton, Ann. Rev. Mar. Sci., 10(1), 43–69, doi:10.1146/annurev-marine-121916-063126, 2018.

Moreno, A. R., Hagstrom, G. I., Primeau, F. W., Levin, S. A. and Martiny, A. C.: Marine phytoplankton stoichiometry mediates nonlinear interactions between nutrient supply, temperature, and atmospheric CO2, Biogeosciences, 15(9), 2761–2779, doi:10.5194/bg-15-2761-2018, 2018.

Mousing, E. A., Ellegaard, M. and Richardson, K.: Global patterns in phytoplankton community size structure -evidence for a direct temperature effect, Mar. Ecol. Prog. Ser., 497, 25–38, doi:10.3354/meps10583, 2014.

Mouw, C. B., Barnett, A., McKinley, G. A., Gloege, L. and Pilcher, D.: Global ocean particulate organic carbon flux merged with satellite parameters, Earth Syst. Sci. Data, 8(2), 531–541, doi:10.5194/essd-8-531-2016, 2016a.

Mouw, C. B., Barnett, A., McKinley, G. A., Gloege, L. and Pilcher, D.: Phytoplankton size impact on export flux in the global ocean, Global Biogeochem. Cycles, 30(10), 1542–1562, doi:10.1002/2015GB005355, 2016b.

Nagelkerken, I. and Connell, S. D.: Global alteration of ocean ecosystem functioning due to increasing human CO2 emissions, Proc. Natl. Acad. Sci. U. S. A., 112(43), 13272–13277, doi:10.1073/pnas.1510856112, 2015.

Niemeyer, D., Kemena, T. P., Meissner, K. J. and Oschlies, A.: A model study of warming-induced phosphorus-oxygen feedbacks in open-ocean oxygen minimum zones on millennial timescales, Earth Syst. Dyn., 8(2), 357–367, doi:10.5194/esd-8-357-2017, 2017.

Niemeyer, D., Kriest, I. and Oschlies, A.: The effect of marine aggregate parameterisations on nutrients and oxygen minimum zones in a global biogeochemical model, Biogeosciences, 16(15), 3095–3111, doi:10.5194/bg-16-3095-2019, 2019.

Norris, R. D., Kirtland Turner, S., Hull, P. M. and Ridgwell, A.: Marine ecosystem responses to Cenozoic global change, Science, 341(6145), 492–498, doi:10.1126/science.1240543, 2013.

Olivarez Lyle, A. and Lyle, M. W.: Missing organic carbon in Eocene marine sediments: Is metabolism the biological feedback that maintains end-member climates?, Paleoceanography, 21(PA2007), 1–13, doi:10.1029/2005PA001230, 2006.

Omand, M. M., Govindarajan, R., He, J. and Mahadevan, A.: Sinking flux of particulate organic matter in the oceans: Sensitivity to particle characteristics, Sci. Rep., 10(1), 1–16, doi:10.1038/s41598-020-60424-5, 2020.

Pasquier, B. and Holzer, M.: The plumbing of the global biological pump: Efficiency control through leaks, pathways, and time scales, J. Geophys. Res. Ocean., 121(8), 6367–6388, doi:10.1002/2016JC011821, 2016.

Pershing, A. J., Christensen, L. B., Record, N. R., Sherwood, G. D. and Stetson, P. B.: The impact of whaling on the ocean carbon cycle: Why bigger was better, PLoS One, 5(8), 1–9, doi:10.1371/journal.pone.0012444, 2010.

Pomeroy, L. R. and Wiebe, W. J.: Temperature and substrates as interactive limiting factors for marine heterotrophic bacteria, Aquat. Microb. Ecol., 23(2), 187–204, doi:10.3354/ame023187, 2001.

Quere, C. Le, Harrison, S. P., Colin Prentice, I., Buitenhuis, E. T., Aumont, O., Bopp, L., Claustre, H., Cotrim Da Cunha, L., Geider, R., Giraud, X., Klaas, C., Kohfeld, K. E., Legendre, L., Manizza, M., Platt, T., Rivkin, R. B., Sathyendranath, S., Uitz, J., Watson, A. J. and Wolf-Gladrow, D.: Ecosystem dynamics based on plankton functional types for global ocean biogeochemistry models, Glob. Chang. Biol., (2005), 051013014052005-???, doi:10.1111/j.1365-2486.2005.1004.x, 2005.

Raupach, M. R., Gloor, M., Sarmiento, J. L., Canadell, J. G., Frölicher, T. L., Gasser, T., Houghton, R. A., Le Quéré, C. and Trudinger, C. M.: The declining uptake rate of atmospheric CO2 by land and ocean sinks, Biogeosciences, 11(13), 3453–3475, doi:10.5194/bg-11-3453-2014, 2014.

Redfield, A. C.: On the proportions of organic derivatives in sea water and their relation to the composition of plankton, James Johnstone Meml. Vol., 176, 176–192, 1934.

Regaudie-de-Gioux, A. and Duarte, C. M.: Temperature dependence of planktonic metabolism in the ocean, Global Biogeochem. Cycles, 26(1), n/a-n/a, doi:10.1029/2010GB003907, 2012.

Regaudie-De-Gioux, A. and Duarte, C. M.: Temperature dependence of planktonic metabolism in the ocean, Global Biogeochem. Cycles, 26(1), 1–10, doi:10.1029/2010GB003907, 2012.

Richardson, K. and Bendtsen, J.: Photosynthetic oxygen production in a warmer ocean: the Sargasso Sea as a case study, Philos. Trans. R. Soc. A Math. Phys. Eng. Sci., 375(2102), 20160329, doi:10.1098/rsta.2016.0329, 2017.

Richardson, K. and Bendtsen, J.: Vertical distribution of phytoplankton and primary production in relation to nutricline depth in the open ocean, Mar. Ecol. Prog. Ser., 620, 33–46, doi:10.3354/meps12960, 2019.

Ridgwell, A. J. and Schmidt, D. N.: Past constraints on the vulnerability of marine calcifiers to massive carbon dioxide release, Nat. Geosci., 3(3), 196–200, doi:10.1038/ngeo755, 2010.

Ridgwell, A. J., Hargreaves, J. C., Edwards, N. R., Annan, J. D., Lenton, T. M., Marsh, R., Yool, A. and Watson, A.: Marine geochemical data assimilation in an efficient Earth System Model of global biogeochemical cycling, Biogeosciences, 4(1), 87–104, doi:10.5194/bg-4-87-2007, 2007.

Riebesell, U., Schulz, K. G., Bellerby, R. G. J., Botros, M., Fritsche, P., Meyerhöfer, M., Neill, C., Nondal, G., Oschlies, A., Wohlers, J. and Zöllner, E.: Enhanced biological carbon consumption in a high CO2 ocean, Nature, 450(7169), 545–548, doi:10.1038/nature06267, 2007.

Riebesell, U., Rtzinger, A. K. and Oschlies, A.: Sensitivities of marine carbon fluxes to ocean change, Proc. Natl. Acad. Sci. U. S. A., 106(49), 20602–20609, doi:10.1073/pnas.0813291106, 2009.

Sarmento, H., Montoya, J. M., Vázquez-Domínguez, E., Vaqué, D. and Gasol, J. M.: Warming effects on marine microbial food web processes: How far can we go when it comes to predictions?, Philos. Trans. R. Soc. B Biol. Sci., 365(1549), 2137–2149, doi:10.1098/rstb.2010.0045, 2010.

Sarmiento, J. L., Slater, R., Barber, R., Bopp, L., Doney, S. C., Hirst, A. C., Kleypas, J., Matear, R., Mikolajewicz, U., Monfray, P., Soldatov, V., Spall, S. A. and Stouffer, R.: Response of ocean ecosystems to climate warming, Global Biogeochem. Cycles, 18(3), doi:10.1029/2003GB002134, 2004.

Sauerland, V., Kriest, I., Oschlies, A. and Srivastav, A.: Multiobjective Calibration of a Global Biogeochemical Ocean Model

Against Nutrients, Oxygen, and Oxygen Minimum Zones, J. Adv. Model. Earth Syst., 11(5), 1285–1308, doi:10.1029/2018MS001510, 2019.

Schartau, M., Wallhead, P., Hemmings, J., Löptien, U., Kriest, I., Krishna, S., Ward, B. A., Slawig, T. and Oschlies, A.: Reviews and syntheses: Parameter identification in marine planktonic ecosystem modelling, Biogeosciences, 14(6), 1647–1701, doi:10.5194/bg-14-1647-2017, 2017.

Schwinger, J., Tjiputra, J. F., Heinze, C., Bopp, L., Christian, J. R., Gehlen, M., Ilyina, T., Jones, C. D., Salas-Mélia, D., Segschneider, J., Séférian, R. and Totterdell, I.: Nonlinearity of ocean carbon cycle feedbacks in CMIP5 earth system models, J. Clim., 27(11), 3869–3888, doi:10.1175/JCLI-D-13-00452.1, 2014.

Séférian, R., Berthet, S., Yool, A., Palmiéri, J., Bopp, L., Tagliabue, A., Kwiatkowski, L., Aumont, O., Christian, J., Dunne, J., Gehlen, M., Ilyina, T., John, J. G., Li, H., Long, M. C., Luo, J. Y., Nakano, H., Romanou, A., Schwinger, J., Stock, C., Santana-Falcón, Y., Takano, Y., Tjiputra, J., Tsujino, H., Watanabe, M., Wu, T., Wu, F. and Yamamoto, A.: Tracking Improvement in Simulated Marine Biogeochemistry Between CMIP5 and CMIP6, Curr. Clim. Chang. Reports, 6(3), 95–119, doi:10.1007/s40641-020-00160-0, 2020.

Segschneider, J. and Bendtsen, J.: Temperature-dependent remineralization in a warming ocean increases surface pCO2 through changes in marine ecosystem composition, Global Biogeochem. Cycles, 27(4), 1214–1225, doi:10.1002/2013GB004684, 2013.

Shimoda, Y. and Arhonditsis, G. B.: Phytoplankton functional type modelling: Running before we can walk? A critical evaluation of the current state of knowledge, Ecol. Modell., 320, 29–43, doi:10.1016/j.ecolmodel.2015.08.029, 2016.

Sinha, B., Buitenhuis, E. T., Quéré, C. Le and Anderson, T. R.: Comparison of the emergent behavior of a complex ecosystem model in two ocean general circulation models, Prog. Oceanogr., 84(3–4), 204–224, doi:10.1016/j.pocean.2009.10.003, 2010.

Somes, C. J., Landolfi, A., Koeve, W. and Oschlies, A.: Limited impact of atmospheric nitrogen deposition on marine productivity due to biogeochemical feedbacks in a global ocean model, Geophys. Res. Lett., 43(9), 4500–4509, doi:10.1002/2016GL068335, 2016.

Steffen, W., Rockström, J., Richardson, K., Lenton, T. M., Folke, C., Liverman, D., Summerhayes, C. P., Barnosky, A. D., Cornell, S. E., Crucifix, M., Donges, J. F., Fetzer, I., Lade, S. J., Scheffer, M., Winkelmann, R. and Schellnhuber, H. J.: Trajectories of the Earth System in the Anthropocene, Proc. Natl. Acad. Sci., 115(33), 8252–8259, doi:10.1073/pnas.1810141115, 2018.

Stramma, L., Johnson, G. C., Sprintall, J. and Mohrholz, V.: Expanding oxygen-minimum zones in the tropical oceans, Science, 320(5876), 655–658, doi:10.1126/science.1153847, 2008.

Tagliabue, A., Bopp, L. and Gehlen, M.: The response of marine carbon and nutrient cycles to ocean acidification: Large uncertainties related to phytoplankton physiological assumptions, Global Biogeochem. Cycles, 25(3), 1–13, doi:10.1029/2010GB003929, 2011.

Tagliabue, A., Aumont, O., DeAth, R., Dunne, J. P., Dutkiewicz, S., Galbraith, E., Misumi, K., Moore, J. K., Ridgwell, A.,

Sherman, E., Stock, C., Vichi, M., Völker, C. and Yool, A.: How well do global ocean biogeochemistry models simulate dissolved iron distributions?, Global Biogeochem. Cycles, 30(2), 149–174, doi:10.1002/2015GB005289, 2016.

Taucher, J. and Oschlies, A.: Can we predict the direction of marine primary production change under global warming?, Geophys. Res. Lett., 38(2), 1–6, doi:10.1029/2010GL045934, 2011.

Ward, B. A., Dutkiewicz, S. and Follows, M. J.: Modelling spatial and temporal patterns in size-structured marine plankton communities: top–down and bottom–up controls, J. Plankton Res., 36(1), 31–47, doi:10.1093/plankt/fbt097, 2014.

Ward, B. A., Wilson, J. D., Death, R. M., Monteiro, F. M., Yool, A. and Ridgwell, A.: EcoGEnIE 1.0: plankton ecology in the cGEnIE Earth system model, Geosci. Model Dev., 11(10), 4241–4267, doi:10.5194/gmd-11-4241-2018, 2018.

Watson, A. J.: Oxygen crises in the North Adriatic, Science, 354(6319) [online] Available from: http://othes.univie.ac.at/3813/, 2016.

Weber, T., Cram, J. A., Leung, S. W., DeVries, T. and Deutsch, C.: Deep ocean nutrients imply large latitudinal variation in particle transfer efficiency, Proc. Natl. Acad. Sci. U. S. A., 113(31), 8606–8611, doi:10.1073/pnas.1604414113, 2016.

Wilson, J. D., Barker, S. and Ridgwell, A.: Assessment of the spatial variability in particulate organic matter and mineral sinking fluxes in the ocean interior: Implications for the ballast hypothesis, Global Biogeochem. Cycles, 26(4), n/a-n/a, doi:10.1029/2012GB004398, 2012.

Wilson, J. D., Monteiro, F., Schmidt, D. N., Ward, B. A. and Ridgwell, A.: Linking marine plankton ecosystems and climate: A new modelling approach to the warm Early Eocene climate., Paleoceanogr. Paleoclimatology, doi:10.1029/2018PA003374, 2018.

Yao, W., Kvale, K. F., Achterberg, E., Koeve, W. and Oschlies, A.: Hierarchy of calibrated global models reveals improved distributions and fluxes of biogeochemical tracers in models with explicit representation of iron, Environ. Res. Lett., 14(11), doi:10.1088/1748-9326/ab4c52, 2019.

Zeebe, R. E. and Wolf-Gladrow, D.: CO2 in Seawater: Equilibrium, Kinetics, Isotopes, Elsevier Oceanography Series (65)., 2001.

Figures and Tables

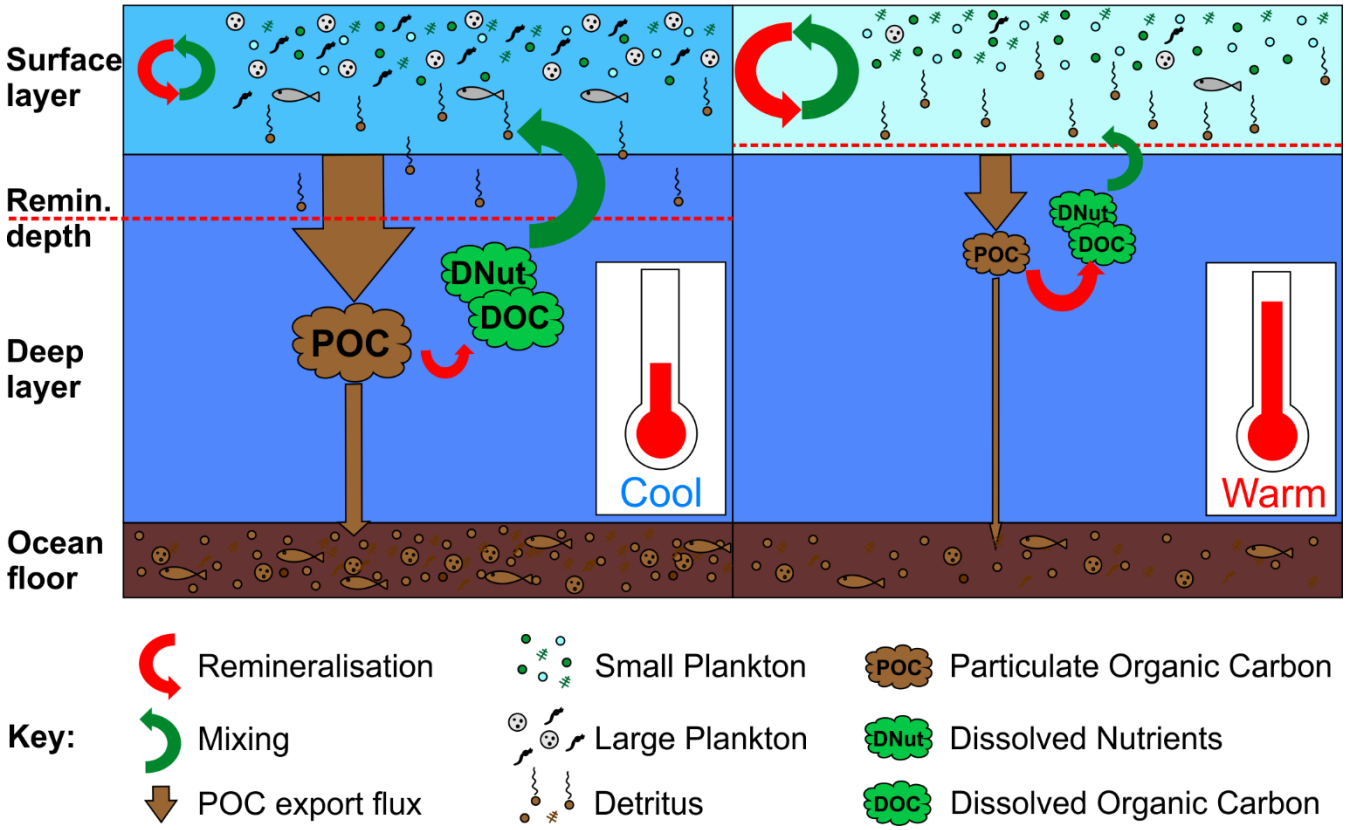

Figure 1: Schematic illustrating the impact of warming on the soft tissue biological pump. On the left-side, under cooler preindustrial conditions cGEnIE's surface layer remains fairly well mixed with the deep ocean (green arrow), returning dissolved nutrients and carbon (DNut & DOC) from remineralisation of exported POC (red arrow), while some POC is remineralised above the remineralisation depth (surface red arrows) partly within the surface layer. On the right-side, warming leads to a shift to dominance by smaller plankton as well as stratification leading to less mixing between the shallow and deep ocean, while shoaling of the remineralisation depth leads to greater recycling of nutrients and carbon close to the surface layer, combining to result in an overall reduction in POC export and sedimentation.

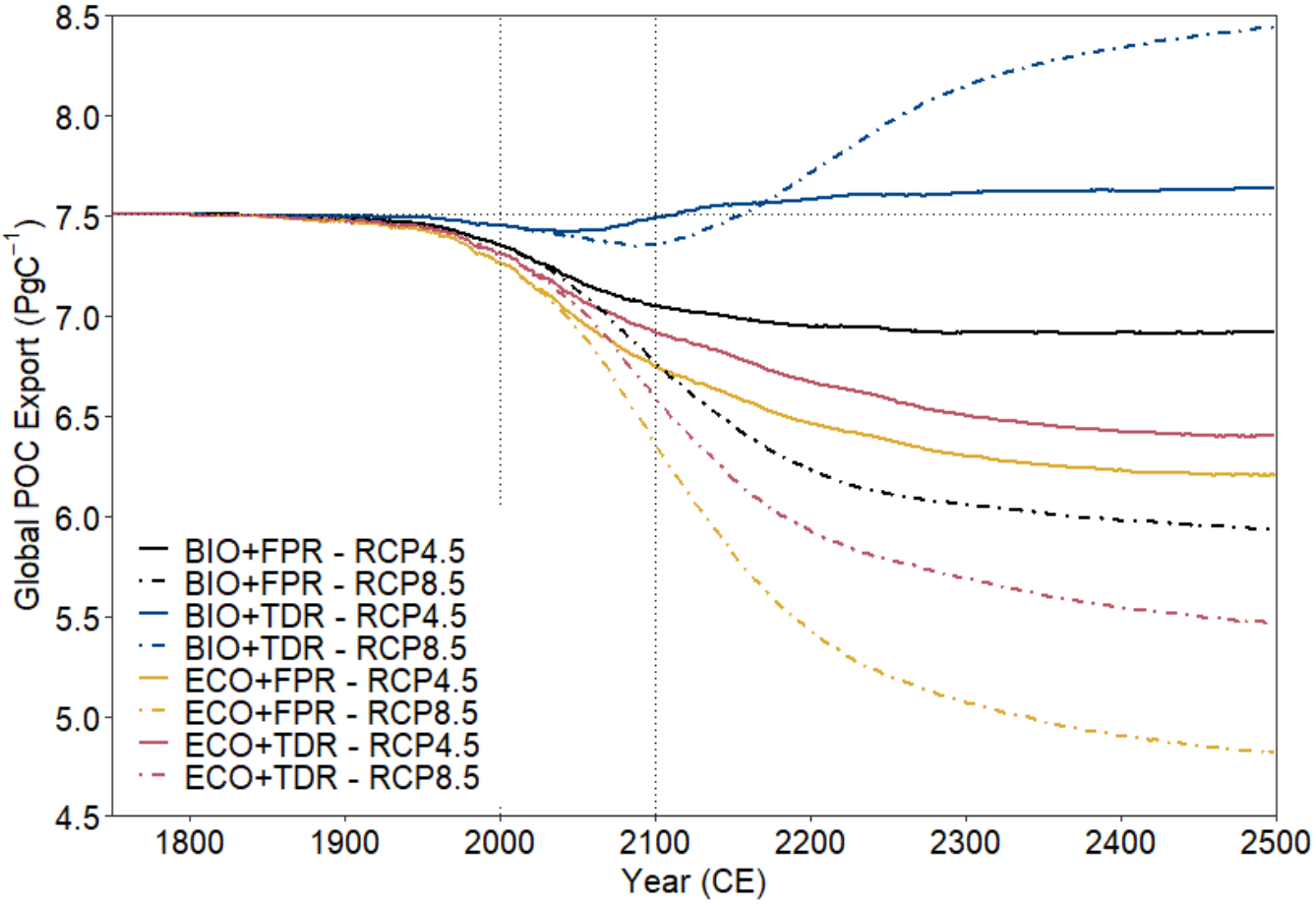

Figure 2: cGEnIE/ecoGEnIE simulation results for global POC export flux under different configurations and forcing scenarios. Results for RCP4.5 (solid lines) and RCP8.5 (dot-dashed lines) are shown for each of the configurations (BIO+FPR – black; BIO+TDR – blue; ECO+FPR – yellow; ECO+TDR – red), and the baseline POC export and the 21st Century marked by the horizontal and vertical dotted lines respectively. Results for all emission scenarios are shown in Supplementary Figure S21.

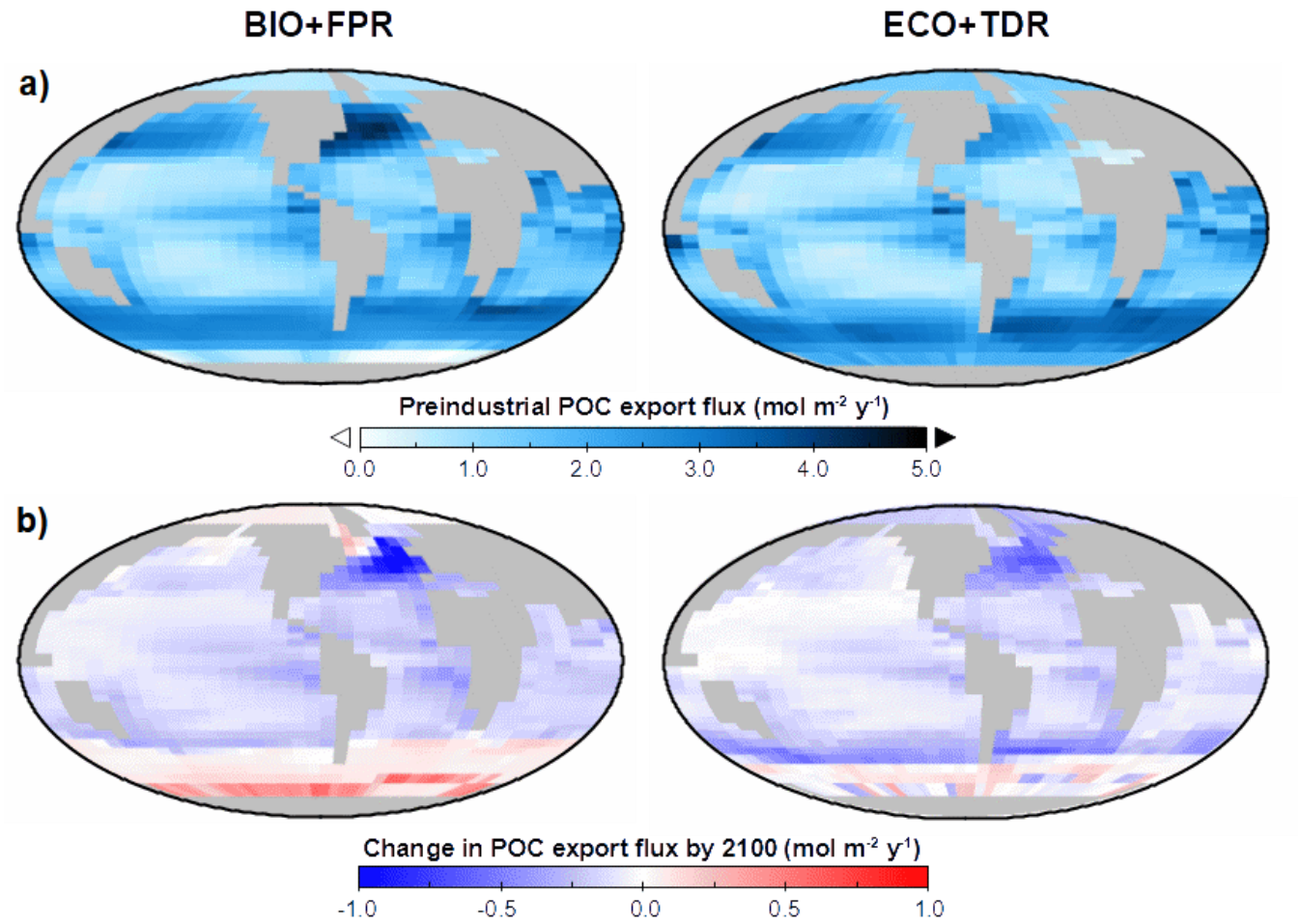

Figure 3: a) cGEnIE POC export maps for BIO+FPR (left) and ECO+TDR (right), showing baseline export patterns. b) The change in POC export by 2100 relative to the 1765 preindustrial baseline as a result of RCP4.5 for BIO+FPR (left) and ECO+TDR (right).

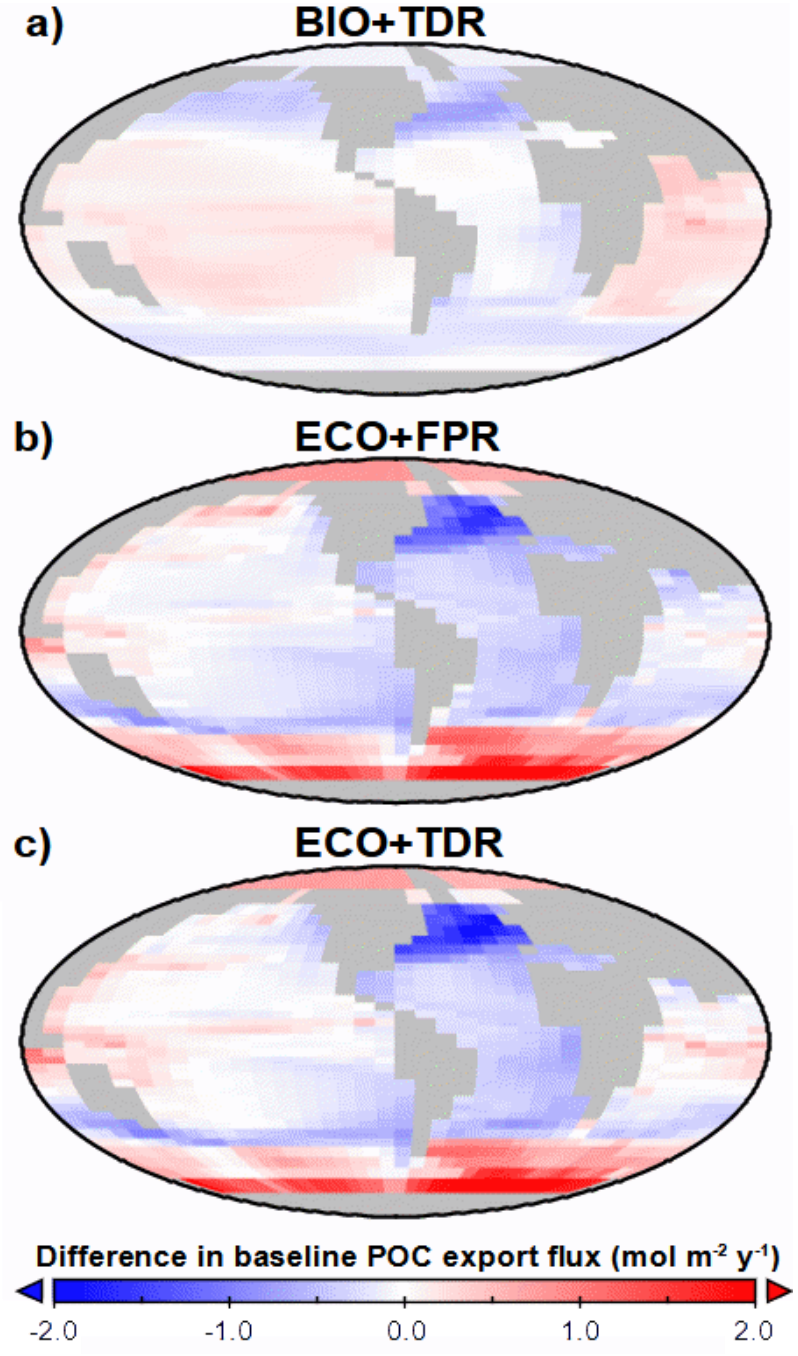

Figure 4: cGEnIE/ecoGEnIE POC export maps, showing changes in baseline for BIO+TDR (a), ECO+FPR (b), and ECO+TDR (c) relative to the default BIO+FPR configuration (Figure 3, left).

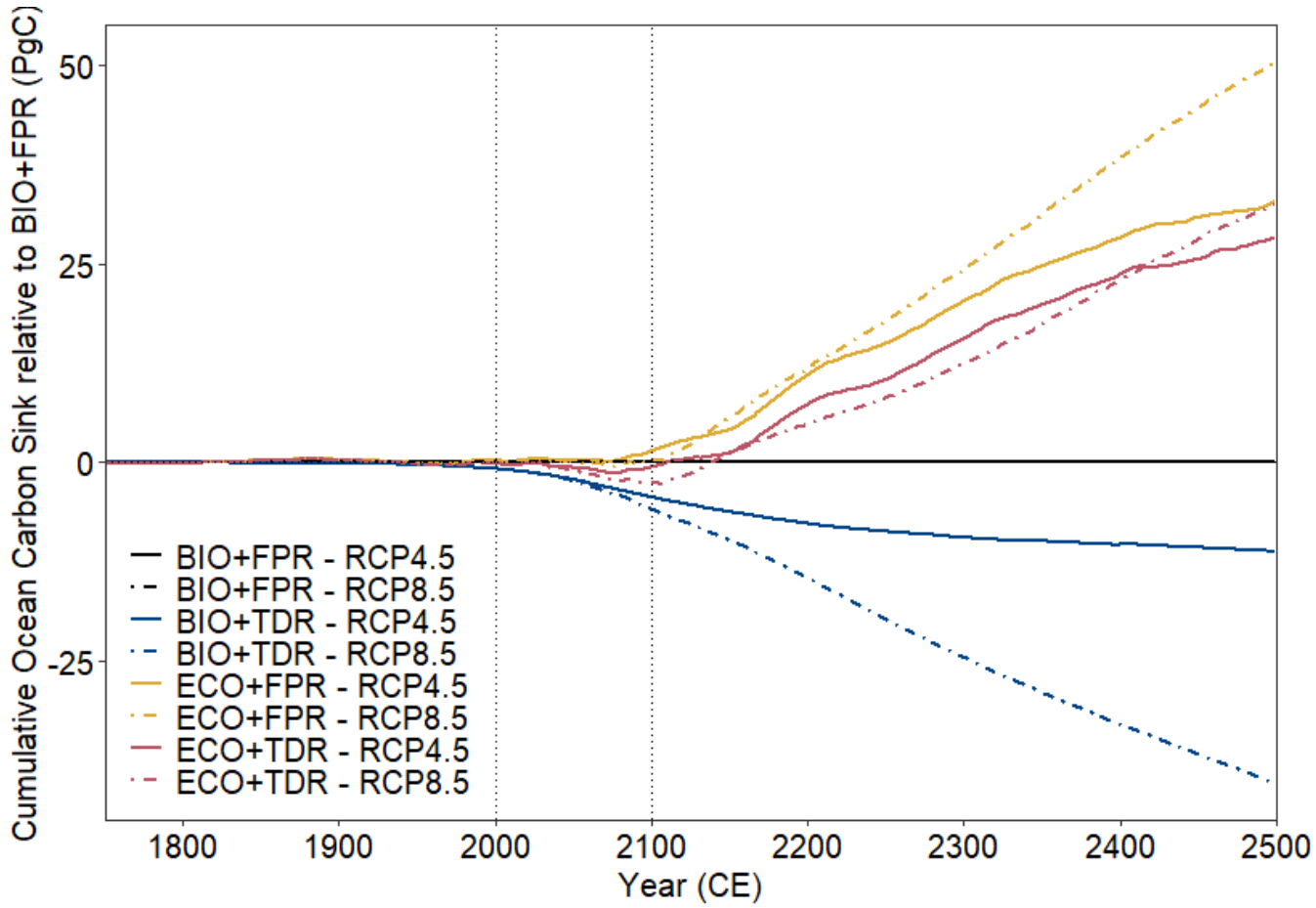

Figure 5: cGEnIE/ecoGEnIE simulation results for cumulative ocean carbon sink relative to BIO+FPR under different configurations and forcing scenarios. Results for RCP4.5 (solid lines) and RCP8.5 (dot-dashed lines) are shown for each of the configurations (BIO+FPR – black; BIO+TDR – blue; ECO+FPR – yellow; ECO+TDR – red), and the 21st Century marked by the vertical dotted lines.

Table 1: Features critical for resolving biological pump dynamics of CMIP5 ESMs used to simulate ocean carbon sink projections in IPCC AR5. Details based on IPCC AR5 WG1 Table 6.11, Table 9.A.1, and cited literature. Note that there are some mismatches between number of functional groups reported in the literature and the IPCC description. Highlighted cells indicate the models with the most (**) or moderately (*) comprehensive – but not necessarily sufficient – representation of the relevant model feature.

ES Model (variant)	BGCM module	Key references	Type ※	Functional Groups †	Remineral-isation ‡	Element Cycles §	Elemental Stoichiometry ǀ	Limiting Nutrient	Shell Si/Ca ◊	Ballasting option ⁋
BCC-CSM1.1	(Inc.)	Based on OCMIP2 & MOM4; (Najjar et al., 2007; Wu et al., 2014)	Nutrient-restoring	0T: N/A [0]	Fixed rate	C, P, O	Fixed	P	N/A	N/A
CESM1 (BGC)	BEC	(Long et al., 2013; Moore et al., 2013)	**PFTs	**4.5T: 3.5P (diatom, diazo., small + cocco. fraction) 1Z [4]	Fixed rate (soft / ballast)	**C, N, P, Fe, Si, O	*Fixed quasi-Redfield (except diaz), Fe quota	**N, P, Fe, Si	**Diatoms (Si) & Coccos (Ca) separated by classes	*Yes, part of fixed remin. rate
CanESM2	CMOC	(Arora et al., 2009, 2011; Christian et al., 2010)	NPZD	2T: 1P 1Z [1X]	**TDR	C, N	Fixed - Redfield	N, (Fe-param'd)	Temp-depend rain ratio for Ca, no Si	No mention
GFDL-ESM (2G & 2M)	TOPAZ2	(Dunne et al., 2012, 2013; Henson et al., 2009)	**PFTs	**3.5T: 3P (small, large, diazo.) 1Z implicit [6X]	Fixed rate (an/oxic)	**C, N, P, Fe, Si, O	**Variable N:P, optimal allocation, PFe quota	**N + Am, P, Fe	*No classes; opal (Si), calc., & arag.(Ca) "diagnosed"	**Yes
HADGEM 2 (CC & ES)	Diat-HadOCC	(Collins et al., 2011; Halloran, 2012; Jones et al., 2011; Palmer and Totterdell, 2001)	**PFTs	*3T: 2P (non/diatoms) 1Z [3]	Fixed rate	C, N, Fe, Si	Fixed - Redfield	*N, Fe, Si (& DMS)	**Si/Ca separated as diatom/non classes	No mention
INM-CM4	(Inc.)	(Volodin, 2007)	Paramet-erised POC flux	0T: N/A [0]	N/A	C	N/A	N/A	N/A	N/A
IPSL-CM5 (A-LR, A-MR, & B-LR)	PISCES	(Aumont et al., 2003; Aumont and Bopp, 2006; Dufresne et al., 2013)	**PFTs	**4T: 2P (diatom, nano) 2Z (micro, meso) [2X]	Fixed rate (an/oxic)	**C, N, P, Fe, Si	*C,N,P Redfield; Fe,Si quota	**N + Am, P, Fe, Si	**Diatom Si class; ad hoc parametrised Rain Ratio for Ca	No
MIROC. ESM (- & CHEM)	(NPZD-type)	(Kawamiya et al., 2000; Schmittner et al., 2005; Watanabe et al., 2011)	NPZD	2T: 1P 1Z [2]	Fixed rate	C, N	Fixed - Redfield	N	N/A	No mention
MPI-ESM (LR)	HAMOC C5	(Ilyina et al., 2013)	NPZD	2T: 1P 1Z [2]	Fixed rate (an/oxic)	**C, N, P, Fe, Si	Fixed - Redfield	**N, P, Fe	*Si/Ca fractionated by Si availability	No mention
NorESM1 (ME)	HAMOC C5	(Tjiputra et al., 2013)								

※ NPZD = Nutrient Phytoplankton Zooplankton Detritus pools; PFTs = Plankton Functional Types (diatoms, coccolithopores, etc.)

† #T:=No. Total; #P=No. Phytoplankton types; #Z= No. Zooplankton types; [#]= IPCC AR5.1 table 6.11 No. plankton types; [#X]= mismatch between cited literature and IPCC AR5.1 Table 6.11

‡ Fixed rate = prescribed remineralisation profile for sinking POC (sometimes split by class); TDR= temperature-dependent remineralisation

§ Major & minor nutrient cycles present

| Fixed= set ratio of C:N:P etc. (e.g. Redfield Ratio) in OM; Variable/quota= OM can take up / store differing ratios of nutrient relative to C

¶ One major limiting nutrient (P or N), co-limitation by both, and/or micronutrients (e.g. Fe) as well. Am=ammonium

◊ Silicifiers & calcifiers differentiated (& by parameterisation or by functional classes)

⁋ Ballasting (OM sticks to sinking heavy PIC) available as an option. N/A means not applicable (model type does not allow ballasting to be parameterised); No mention means ballasting is not mentioned in the key references (implying ballasting is not available).

Table 2: Simulated changes in POC export and air-to-sea CO_2 flux by 2100 CE under different climate scenarios (CMIP5 RCPs 3PD, 4.5, 6.0, and 8.5), illustrating the relative changes in biological pump strength and ocean carbon sink capacity respectively.

Climate scenario (CMIP5 RCP)	Model Configur-ation	Biological Pump Strength			Ocean Carbon Sink Capacity	
		POC export in 2100 (PgC) *(% change vs. preindustrial)*	Cumulative ΔPOC export by 2100 relative to preindustrial rates (PgC) *(%)*	Cumulative ΔPOC export by 2100 relative to BIO+FPR (PgC) *(%)*	Cumulative Air-to-Sea CO_2 transfer by 2100 (PgC) *(% in ocean vs. total)*	Cumulative Air-to-Sea CO_2 transfer by 2100 relative to BIO+FPR (PgC) *(%)*
3PD (low warming, 1.8°C by 2100)	**BIO+FPR**	7.19 *(-4.2%)*	-35.90 *(-4.8%)*	0 *(0%)*	450.1 *(52.4%)*	0 *(0%)*
	BIO+TDR	7.54 *(+0.4%)*	-6.98 *(-0.9%)*	+28.92 *(+3.9%)*	446.6 *(52.0%)*	-3.48 *(-0.8%)*
	ECO+FPR	6.95 *(-7.5%)*	-57.74 *(-7.7%)*	-21.84 *(-2.9%)*	452.5 *(52.7%)*	+2.46 *(+0.5%)*
	ECO+TDR	7.08 *(-5.7%)*	-45.65 *(-6.1%)*	-9.74 *(-1.3%)*	451.0 *(52.5%)*	+0.90 *(+0.2%)*
4.5 (moderate warming, 2.6°C by 2100)	**BIO+FPR**	7.05 *(-6.2%)*	-41.04 *(-5.5%)*	0 *(0%)*	568.4 *(44.3%)*	0 *(0%)*
	BIO+TDR	7.49 *(-0.3%)*	-9.74 *(-1.3%)*	+31.30 *(+4.2%)*	564.1 *(44.0%)*	-4.35 *(-0.8%)*
	ECO+FPR	6.74 *(-10.2%)*	-64.21 *(-8.6%)*	-23.18 *(-3.1%)*	570.0 *(44.4%)*	+1.61 *(+0.3%)*
	ECO+TDR	6.91 *(-7.9%)*	-51.20 *(-6.8%)*	-10.16 *(-1.4%)*	568.1 *(44.3%)*	-0.37 *(-0.1%)*
6.0 (high warming, 3.2°C by 2100)	**BIO+FPR**	6.94 *(-7.6%)*	-42.73 *(-5.7%)*	0 *(0%)*	641.5 *(38.0%)*	0 *(0%)*
	BIO+TDR	7.42 *(-1.2%)*	-11.21 *(-1.5%)*	+31.52 *(+4.2%)*	636.8 *(37.7%)*	-4.81 *(-0.8%)*
	ECO+FPR	6.61 *(-12.0%)*	-66.23 *(-8.8%)*	-23.50 *(-3.1%)*	642.2 *(38.0%)*	+0.82 *(+0.1%)*
	ECO+TDR	6.79 *(-9.5%)*	-53.07 *(-7.1%)*	-10.34 *(-1.4%)*	640.2 *(37.9%)*	-1.43 *(-0.2%)*
8.5 (severe warming, 4.2°C by 2100)	**BIO+FPR**	6.76 *(-9.5%)*	-49.37 *(-6.6%)*	0 *(0%)*	766.3 *(31.5%)*	0 *(0%)*
	BIO+TDR	7.35 *(-2.1%)*	-14.61 *(-1.9%)*	+34.76 *(+4.6%)*	760.5 *(31.3%)*	-5.88 *(-0.8%)*
	ECO+FPR	6.36 *(-15.4%)*	-75.17 *(-10.0%)*	-25.79 *(-3.4%)*	766.7 *(31.5%)*	+0.34 *(+0%)*
	ECO+TDR	6.59 *(-12.3%)*	-60.71 *(-8.1%)*	-11.34 *(-1.5%)*	764.0 *(31.4%)*	-2.33 *(-0.3%)*

905